Title

Extension and magmatism in the Cerocahui basin, northern Sierra Madre Occidental, western Chihuahua, Mexico

Journal

International Geology Review, 57(5-8)

ISSN

0020-6814

Authors

Murray, Bryan P
Busby, Cathy J
de los Angeles Verde Ramírez, María

Publication Date

2015-06-11

DOI

10.1080/00206814.2014.941022

Peer reviewed

International Geology Review, 2014
http://dx.doi.org/10.1080/00206814.2014.941022

Taylor & Francis
Taylor & Francis Group

Extension and magmatism in the Cerocahui basin, northern Sierra Madre Occidental, western Chihuahua, Mexico

Bryan P. Murray[a]*, Cathy J. Busby[a] and María de los Angeles Verde Ramírez[b]

[a]*Department of Earth Science, University of California, Santa Barbara, CA, USA;* [b]*Posgrado en Ciencias de la Tierra, Instituto de Geología, Universidad Nacional Autónoma de México, Ciudad Universitaria, México D.F., Mexico*

(*Received 22 March 2014; accepted 30 June 2014*)

The Sierra Madre Occidental of northwestern Mexico is the biggest silicic large igneous province of the Cenozoic, yet very little is known about its geology due to difficulties of access to much of this region. This study presents geologic maps and two new U-Pb zircon laser ablation inductively coupled plasma mass spectrometry ages from the Cerocahui basin, a previously unmapped and undated ~25 km-long by ~12 km-wide half-graben along the western edge of the relatively unextended core of the northern Sierra Madre Occidental silicic large igneous province. Five stratigraphic units are defined in the study area: (1) undated welded to non-welded silicic ignimbrites that underlie the rocks of the Cerocahui basin, likely correlative to Oligocene-age ignimbrites to the east and west; (2) the ca. 27.5–26 Ma Bahuichivo volcanics, comprising mafic-intermediate lavas and subvolcanic intrusions in the Cerocahui basin; (3) alluvial fan deposits and interbedded distal non-welded silicic ignimbrites of the Cerocahui clastic unit; (4) basalt lavas erupted into the Cerocahui basin following alluvial deposition; and (5) silicic hypabyssal intrusions emplaced along the eastern margin of the basin and to a lesser degree within the basin deposits.

The main geologic structures in the Cerocahui basin and surrounding region are NNW-trending normal faults, with the basin bounded on the east by the syndepositional W-dipping Bahuichivo–Bachamichi and Pañales faults. Evidence of syndepositional extension in the half-graben (e.g. fanning dips, unconformities, coarsening of clastic deposits toward basin-bounding faults) indicates that normal faulting was active during deposition in the Cerocahui basin (Bahuichivo volcanics, Cerocahui clastic unit, and basalt lavas), and may have been active earlier based on regional correlations.

The rocks in the Cerocahui basin and adjacent areas record: (1) the eruption of silicic outflow ignimbrite sheets, likely erupted from caldera sources to the east during the early Oligocene pulse of the mid-Cenozoic ignimbrite flare-up, mostly prior to synextensional deposition in the Cerocahui basin (pre-27.5 Ma); (2) synextensional late Oligocene mafic-intermediate composition magmatism and alluvial fan sedimentation (ca. 27.5–24.5 Ma), which occurred during the lull between the Early Oligocene and early Miocene pulses of the ignimbrite flare-up; and (3) post-extensional emplacement of silicic hypabyssal intrusions along pre-existing normal faults, likely during the early Miocene pulse of the ignimbrite flare-up (younger than ca. 24.5 Ma). The timing of extensional faulting and magmatism in the Cerocahui basin and surrounding area generally coincides with previous models of regional-scale middle Eocene to early Miocene southwestward migration of active volcanism and crustal extension in the northern Sierra Madre Occidental controlled by post-late Eocene (ca. 40 Ma) rollback/fallback of the subducted Farallon slab.

Keywords: Sierra Madre Occidental; Mexico; ignimbrite flare-up; continental extension; synextensional deposition

Introduction

The Sierra Madre Occidental of western Mexico is the third biggest (up to 400,000 km^3) and best-preserved silicic large igneous province in Earth's history and is the largest of the Cenozoic (Figure 1; Bryan 2007; Ferrari *et al.* 2007; Bryan and Ernst 2008; Bryan and Ferrari 2013). Despite its size and preservation, very little is known about the geology of the Sierra Madre Occidental due to difficulties of access to much of this region. A large part of the Sierra Madre Occidental remains unmapped and undated (>90%; Swanson *et al.* 2006), with previous work primarily restricted to the southern region of the igneous province and to the major highways that transverse the northern and central regions (e.g. McDowell and Keizer 1977; Swanson and McDowell 1984, 1985; Wark *et al.* 1990; Aguirre-Díaz and McDowell 1991, 1993; McDowell and Mauger 1994; Ferrari *et al.* 2002; McDowell 2007; McDowell and McIntosh 2012). Owing to increased accessibility to the region, recent studies in the northern Sierra Madre Occidental have focused on the Creel-Divisadero area (Figure 1; Swanson *et al.* 2006) and the Guazapares Mining District region (Figure 2; Murray *et al.* 2013) in southwestern Chihuahua.

The Sierra Madre Occidental silicic large igneous province forms a major component of the extensive mid-Cenozoic ignimbrite flare-up that affected much of the southwestern North American Cordillera from the middle Eocene to late Miocene (e.g. Coney 1978; Armstrong and Ward 1991; Ward 1991; Ferrari *et al.* 2002; Lipman 2007; Cather *et al.* 2009; Henry *et al.* 2010, 2012; Best *et al.* 2013). The mid-Cenozoic ignimbrite flare-up occurred

*Corresponding author. Email: bmurray@umail.ucsb.edu

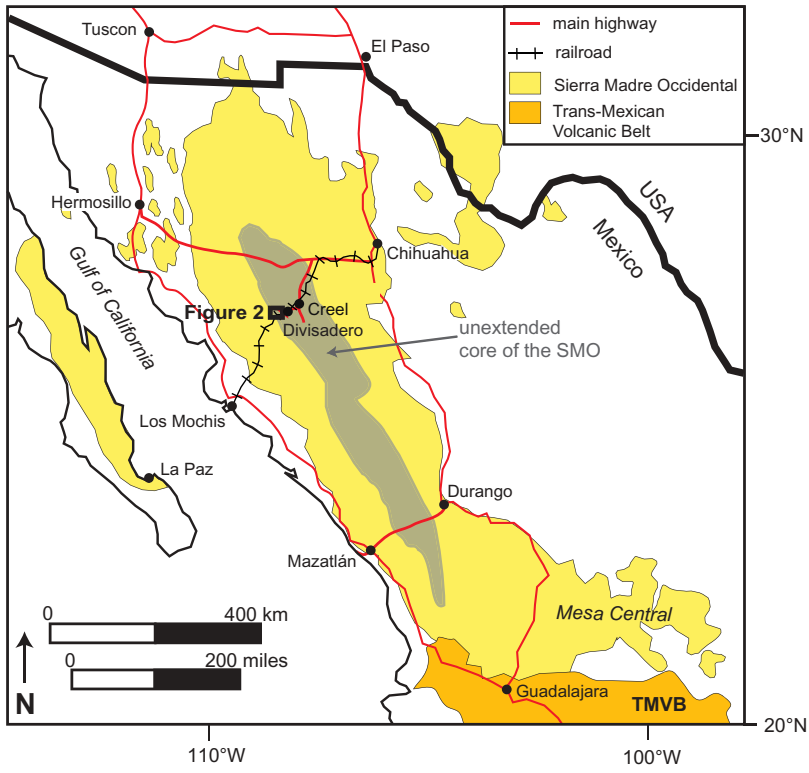

Figure 1. Map of western Mexico showing the extent of the Sierra Madre Occidental (SMO) silicic large igneous province and the unextended core (grey) of the SMO (after Henry and Aranda-Gomez 2000; Ferrari *et al.* 2002; Bryan *et al.* 2013). The location of the study area and the adjacent Guazapares Mining District region, described by Murray *et al.* (2013), is indicated by black box (Figure 2) on the western edge of the unextended core. TMVB, Trans-Mexican Volcanic Belt.

above a subducting slab that progressively fell back and steepened following early Cenozoic low-angle subduction, as suggested by a general westward sweep of volcanism with time (e.g. Best and Christiansen 1991; Dickinson 2006, 2013; Ferrari *et al.* 2007; Henry *et al.* 2010; McQuarrie and Oskin 2010). In western Mexico, Eocene to Miocene slab fallback and arc extension associated with it ultimately led to Miocene rifting in the Gulf of California (Ferrari *et al.* 2007, 2013).

Previous studies suggest that silicic large igneous provinces may initiate as magmatic events in continental regions undergoing broad lithospheric extension, prior to the rupture of continental lithosphere (Bryan et *al.* 2002; Bryan 2007; Best *et al.* 2013; Bryan and Ferrari 2013). In addition, the generation of large silicic magma volumes (e.g. Hildreth 1981) and some very large-magnitude explosive silicic eruptions (Aguirre-Díaz and Labarthe-Hernández 2003; Costa *et al.* 2011) may be favoured by crustal extension. Therefore, studying the relationships between the timing of extensional deformation and magmatism is an important consideration toward understanding the development of the Sierra Madre Occidental.

Here we present new geologic mapping, stratigraphy, and geochronology in a previously unrecognized extensional basin in the northern Sierra Madre Occidental (Figure 1). We refer to this basin as the 'Cerocahui basin' (Figures 2–4; Plate 1, see http://dx.doi.org/10.1080/00206814.2014.941022), and show that it is an extensive and thick section of red beds and mafic-intermediate composition volcanic rocks that accumulated between two major pulses of silicic magmatism during the mid-Cenozoic ignimbrite flare-up in the northern Sierra Madre Occidental. This basin lies in the western part of the (previously defined) unextended core of the northern Sierra Madre Occidental (Figure 1) and the rock exposure and topographic relief in this poorly known region make it an excellent locality for examining the relationships between extensional basin development and silicic large igneous province magmatism in the Sierra Madre Occidental. With these data, we correlate magmatic and extensional events over a broader region than initially described by Murray *et al.* (2013) in the adjacent Guazapares Mining District to the west (Figure 2), and show that the timing of magmatism and synextensional deposition in this region of the northern Sierra Madre Occidental, which includes both the Cerocahui basin and Guazapares Mining District, supports the interpretation that silicic flare-up magmatism migrated southwestward with time across northwestern Mexico and suggests that the eastern limit of the Gulf Extensional Province extends further into the unextended core than previously recognized.

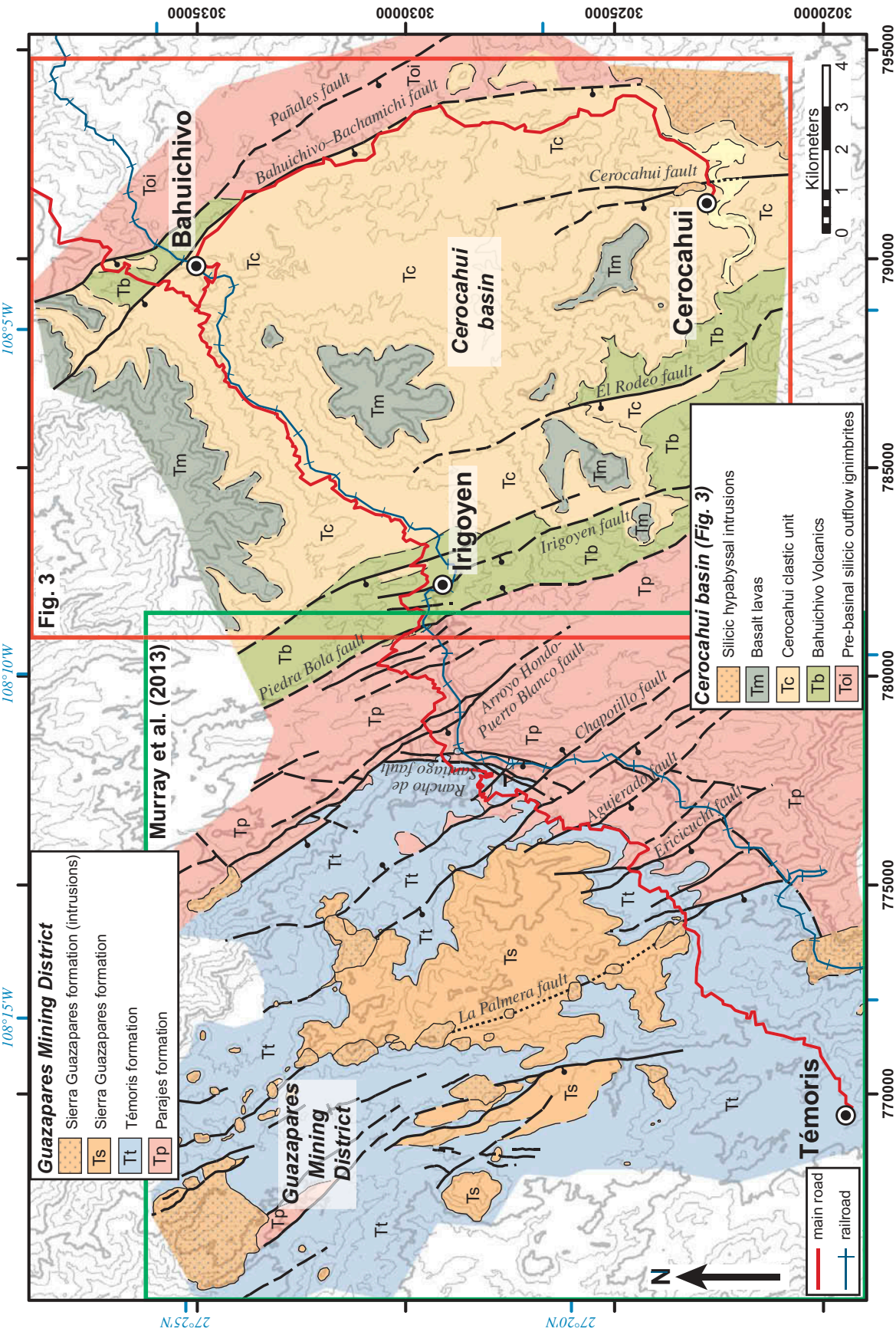

Figure 2. Simplified geologic map of the Cerocahui basin and the adjacent Guazapares Mining District region to the west (green box). The extent of the main lithologic units discussed herein (see Figure 5) and the locations of major faults are shown. The red box indicates the area of the geologic map in Figure 3; detailed maps of the Guazapares Mining District region (green box) are presented in Murray *et al.* (2013). The location of the main roads and the 'Chepe' Copper Canyon railroad that transect the study area are also shown. Map coordinates in black are Universal Transverse Mercator (UTM) zone 12, North American Datum 1927 (NAD27).

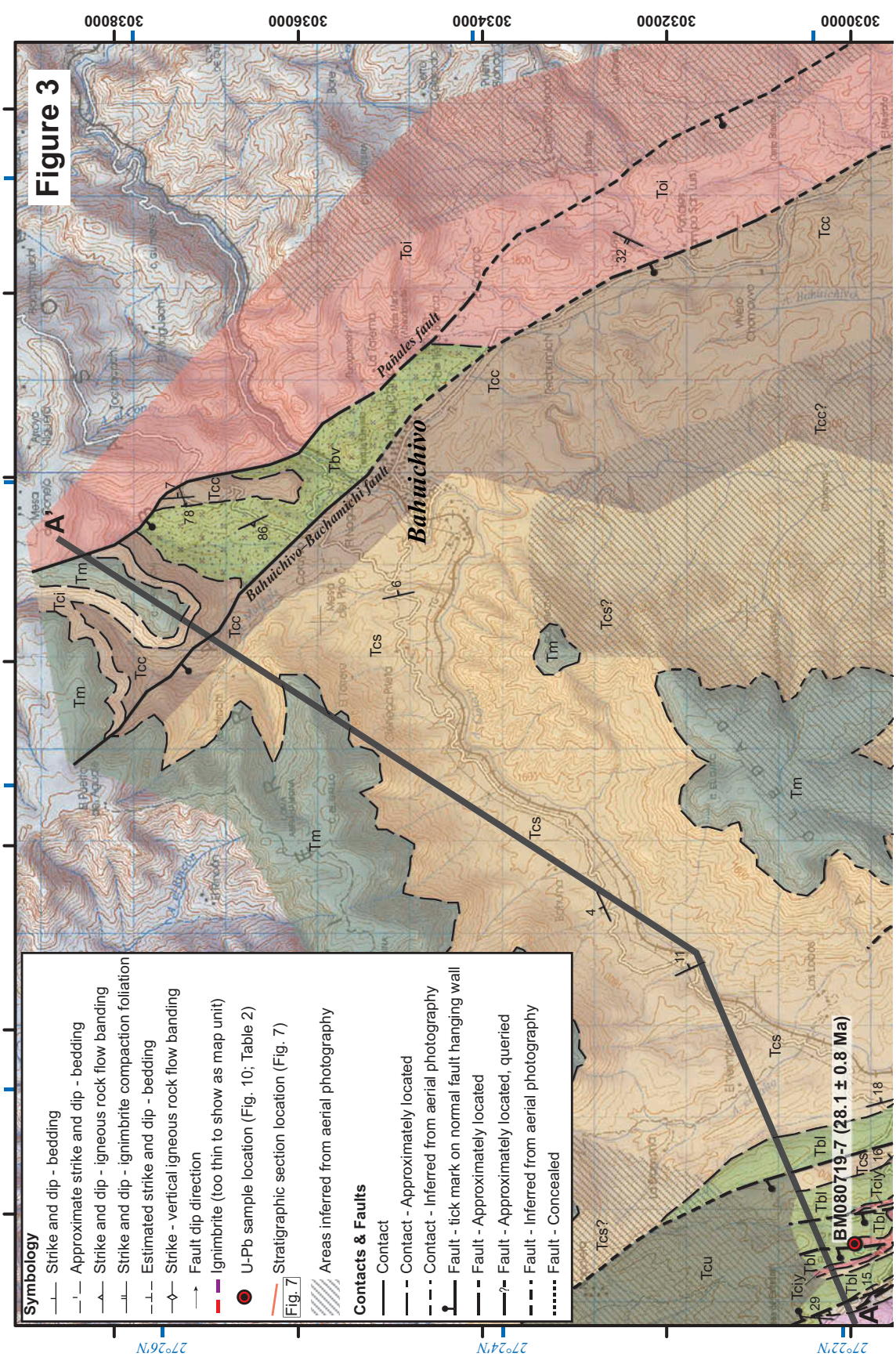

Figure 3. (Continued)

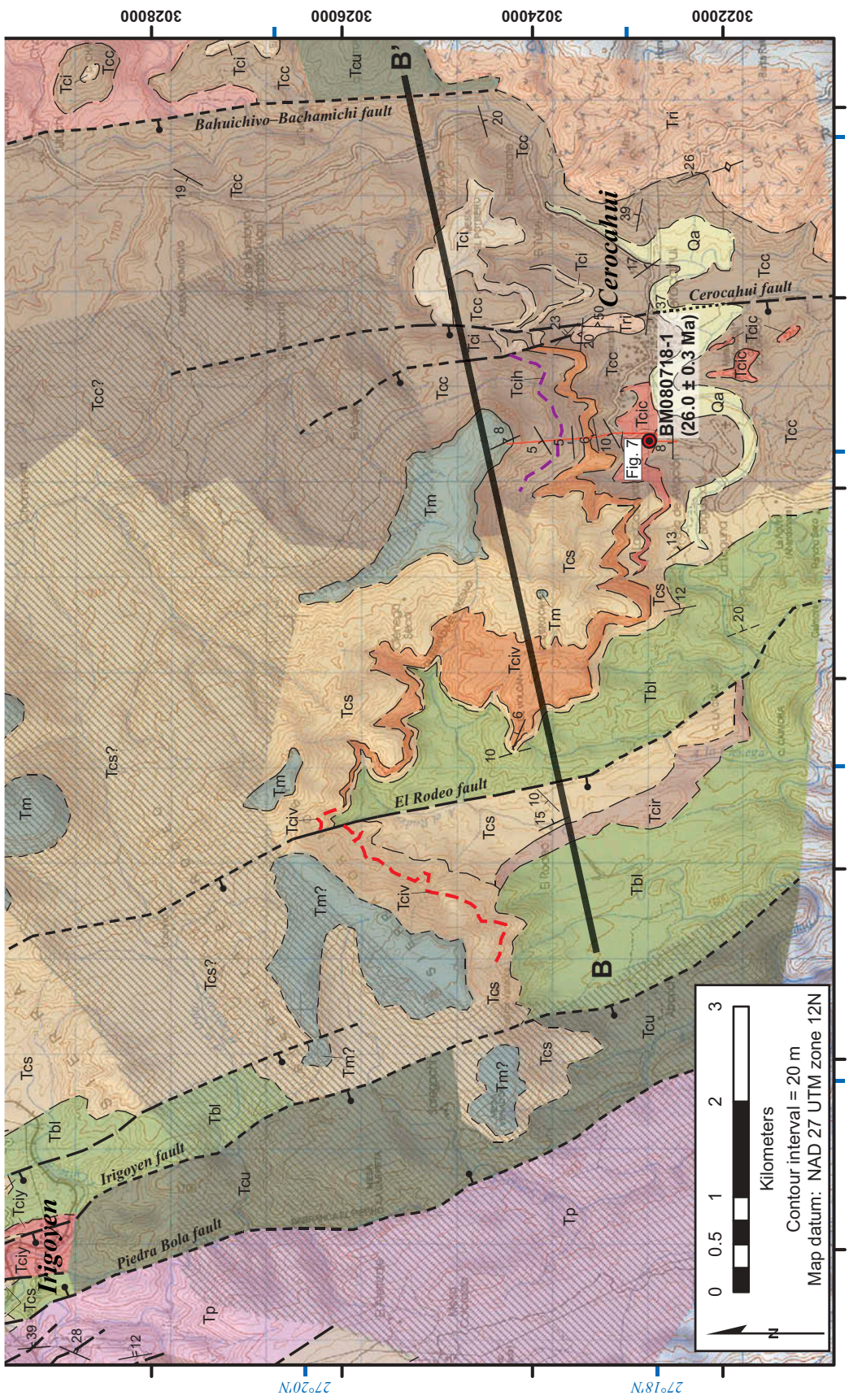

Figure 3. (Continued)

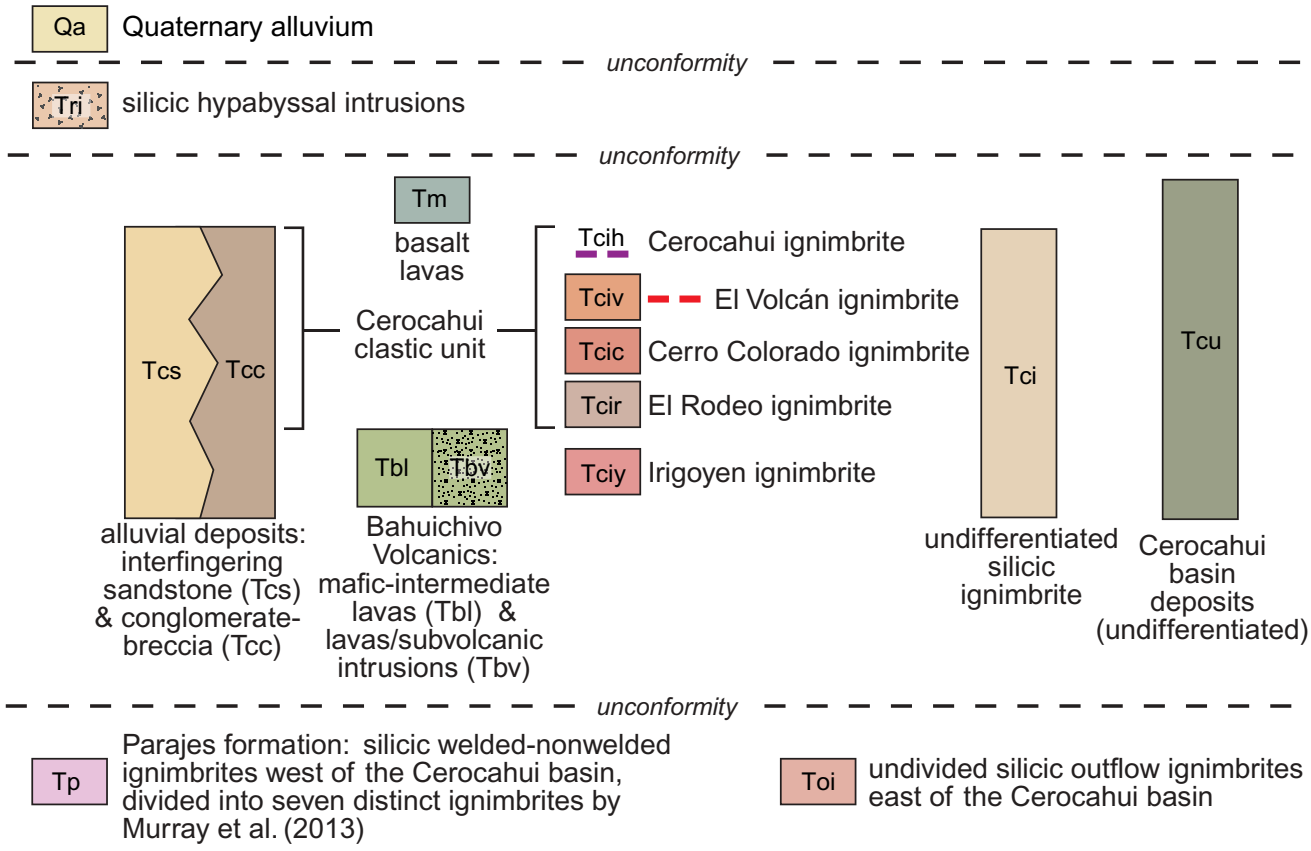

Figure 3. Geologic map of the Cerocahui basin, with lithostratigraphic correlation chart and key for the map units and symbols. The location of cross-sections A and B (Figure 4) and the measured stratigraphic section (Figure 7) are indicated. Much of the basin is inaccessible, with interpretations of the geology in these areas (noted by grey hatch pattern) based on aerial imagery and known geologic relationships from accessible areas. A more detailed (1:24,000) geologic map for the study area is presented in Plate 1. Topographic base map from Instituto Nacional de Estadística, Geografía e Informática (INEGI), original 1:50,000 scale ITRF92 datum projected to NAD27 UTM zone 12 (black coordinates).

Geologic setting

Regional geology

The Sierra Madre Occidental (Figure 1) consists primarily of late Eocene to early Miocene ignimbrites that cover an area of ~400,000 km^2 with an average thickness of 1 km (McDowell and Keizer 1977; McDowell and Clabaugh 1979; Aguirre-Díaz and Labarthe-Hernández 2003; Bryan and Ferrari 2013). There were at least two main pulses of silicic ignimbrite volcanism during the mid-Cenozoic ignimbrite flare-up in the Sierra Madre Occidental, one during the late Eocene–early Oligocene (ca. 36–28 Ma) that occurred throughout the Sierra Madre Occidental and another during the early Miocene (ca. 24–20 Ma) that is generally restricted to the southern part of the igneous province (Ferrari *et al.* 2002, 2007; McDowell and McIntosh 2012). During the final stages of and after each silicic ignimbrite pulse, basaltic andesite lavas, commonly referred to as the Southern Cordillera basaltic andesite province (SCORBA), were intermittently erupted across all of the northern Sierra Madre Occidental (Cameron *et al.* 1989; Ferrari *et al.* 2007).

Following the Laramide orogeny (late Eocene) in western North America, the age distribution of volcanic rocks in the southwestern US and the Sierra Madre Occidental suggests that ignimbrite flare-up magmatism generally migrated southwestward over time (e.g. Coney and Reynolds 1977; Damon *et al.* 1981; Best and Christiansen 1991; Christiansen and Yates 1992; Dickinson 2002, 2006, 2013; Ferrari *et al.* 2007; Henry *et al.* 2010; McQuarrie and Oskin 2010; McDowell 2012; Bryan *et al.* 2013; Busby 2013). This post-Laramide age trend is likely related to removal of the flat to low-angle subducted Farallon plate from the base of the North American plate by either steepening (slab rollback) and/or possible detachment of the deeper part of the subducted slab (e.g. Dickinson and Snyder 1978; Best and Christiansen 1991; Ferrari *et al.* 2007; Henry *et al.* 2010; McQuarrie and Oskin 2010; Best *et al.* 2013; Busby 2013; Dickinson 2013); as a result, commencing by ca. 40 Ma, magmatism migrated southwestward toward the palaeotrench.

The timing of extension in the Sierra Madre Occidental has variably been interpreted to have preceded (e.g. Dreier

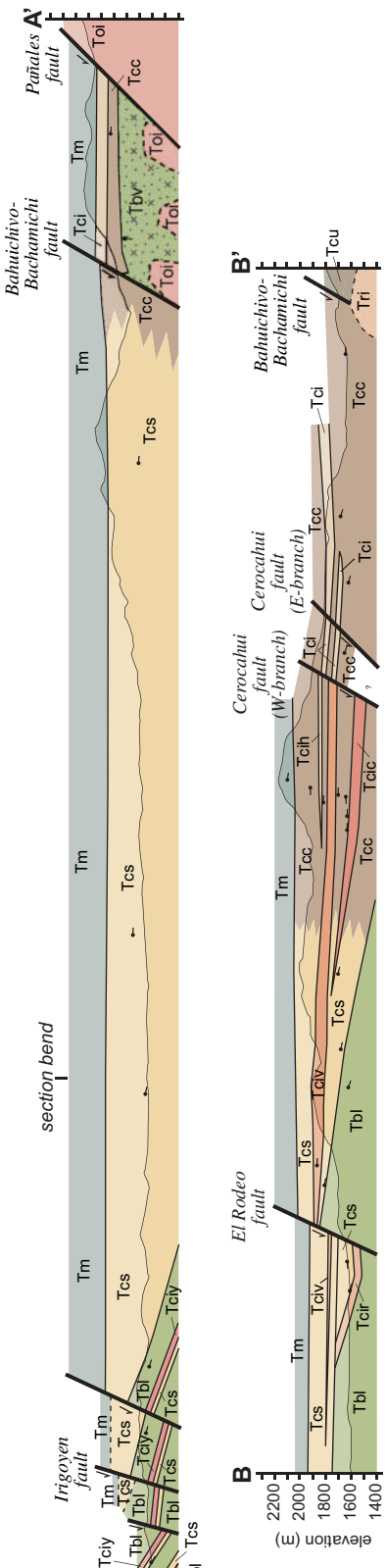

Figure 4. Geologic cross-sections across the northern and southern mapped sections of the Cerocahui basin, with no vertical exaggeration. More detailed (1:24,000) cross-sections for the study area are presented in Plate 1. Rock units inferred above topography are indicated by subdued colour shades. Bedding orientations are indicated by tick marks. See Figure 3 for key to map unit symbols, colours, and cross-section locations. (A) Cross-section A–A' between Irigoyen and Bahuichivo in the northern section of the Cerocahui basin, showing decreased dip of map units upsection and offset of the Cerocahui basin deposits on the western end of the section, resulting in post-depositional tilting of the units across the faults. Mafic-intermediate lavas (Tbl), sandstone, and an undifferentiated silicic ignimbrite (Tci) of the Bahuichivo volcanics are deposited in angular unconformity above the pre-basinal silicic outflow ignimbrites (Tp) on the footwall of the Piedra Bola fault; downdropping of the hanging wall cuts these deposits that onlapped the fault prior to slip, and also steepened bedding on the footwall adjacent to the Piedra Bola fault (drag anticline). (B) Cross-section B–B' between the El Rodeo fault and Cerocahui in the southern section of the Cerocahui basin, showing decreased dip of map units upsection and thickening eastward, suggesting syndepositional extension of the eastern basin-bounding normal fault. Evidence of syndepositional extension of the El Rodeo fault is indicated by the restriction of the El Rodeo ignimbrite (Tcir) to the hanging wall, and the increased thickness and angular unconformity within the Cerocahui clastic unit (Tcs) across the fault.

1984; Ferrari *et al.* 2007), post-dated (e.g. McDowell and Clabaugh 1979; Wark *et al.* 1990; McDowell and Mauger 1994; Gans 1997; McDowell *et al.* 1997; Grijalva-Noriega and Roldán-Quintana 1998; Gans *et al.* 2003), or begun during (e.g. Aguirre-Díaz and McDowell 1993; Luhr *et al.* 2001; Murray *et al.* 2013) the late Eocene–early Oligocene pulse of the ignimbrite flare-up. The eruptions of the Southern Cordillera basaltic andesite (SCORBA) following the early Oligocene ignimbrite pulse have been interpreted as magmatism recording the initiation of regional-scale crustal extension in the northern Sierra Madre Occidental (e.g. Cameron *et al.* 1989; Cochemé and Demant 1991; Gans 1997; McDowell *et al.* 1997; González León *et al.* 2000; Ferrari *et al.* 2007). The central core of the Sierra Madre Occidental is relatively unextended compared to the surrounding late Oligocene- to Miocene-age extensional belts of the southern Basin and Range to the east and the Gulf Extensional Province to the west (Figure 1; Nieto-Samaniego *et al.* 1999; Henry and Aranda-Gomez 2000). Recent studies in the southwestern Sierra Madre Occidental suggest that synvolcanic extension in the Gulf Extensional Province started to develop by the late Oligocene (ca. 30–20 Ma) in an initially wide rift zone, followed by more focused extension in a narrow rift zone around ca. 20–18 Ma that ultimately led to the opening of the Gulf of California (Ferrari *et al.* 2013).

Guazapares Mining District

The recent study of the Guazapares Mining District region near Témoris (Figure 2) to the west of the Cerocahui basin (Murray *et al*. 2013) provides a stratigraphic and structural context for the Cerocahui basin. Three informal formations are recognized in the Guazapares Mining District region (Figure 2). The oldest, the Parajes formation, consists primarily of welded silicic outflow ignimbrite sheets erupted ca. 27.5 Ma, although this formation is likely older based on a possible stratigraphic correlation with the ca. 29.8 Ma Divisadero tuff of Swanson *et al.* (2006). These ignimbrites erupted near the end of the early Oligocene pulse of the ignimbrite flare-up, presumably from calderas of similar age that lie largely to the east of both the Guazapares Mining District (Murray *et al.* 2013) and the Cerocahui basin, described herein. The ca. 27–24.5 Ma Témoris formation (Figure 2), which unconformably overlies the Parajes formation, records local, fault-controlled mafic to intermediate composition magmatism and subsequent distal silicic ignimbrite volcanism, synchronous with extension. Given the similar age and composition, the Témoris formation may be related to the Southern Cordillera basaltic andesite (SCORBA) province erupted in other parts of northern Sierra Madre Occidental following the early Oligocene ignimbrite pulse (Murray *et al.* 2013). The ca. 24.5–23 Ma Sierra Guazapares formation (Figure 2), which overlies the Témoris formation in angular unconformity, records local silicic magmatism, including vent-to-proximal-facies ignimbrite deposits, lavas, and hypabyssal rocks; these were erupted from and intruded into fault-controlled fissure vents within the Guazapares Mining District region. The Sierra Guazapares formation may record the onset of the early Miocene pulse of the mid-Cenozoic ignimbrite flare-up (Murray *et al.* 2013), although this represents much smaller-volume magmatism than the rocks erupted during this pulse in the southern Sierra Madre Occidental (e.g. Ferrari *et al.* 2007).

The main geologic structures in the Guazapares Mining District region are NNW-trending normal faults that bound a series of closely spaced half-graben basins (Figure 2). Growth strata and angular unconformities between each formation indicate that these half-graben basins began to form by the time the upper part of the Parajes formation was erupted (ca. 27.5 Ma) and continued to develop during deposition of the Témoris and Sierra Guazapares formations. In addition, several of these extensional structures controlled the localization of andesitic and silicic volcanic vents and shallow-level intrusions of the Témoris and Sierra Guazapares formations (Murray *et al.* 2013).

The Cerocahui basin

The term ‘Cerocahui basin’ describes the approximately 12 km-wide basin with a mapped length of approximately 25 km (Figures 2 and 3; Plate 1), although it could extend further north and south. It is named for the village of Cerocahui in the southeastern part of the basin, located ~12 km south of the town of Bahuichivo, a stop on the famous ‘Chepe’ Copper Canyon train (Figures 2 and 3; Plate 1). The Cerocahui basin lies on in the western edge of the largely unextended core of the northern Sierra Madre Occidental (Figure 1). Previous work in the Cerocahui basin region has been restricted to regional 1:50,000 and 1:250,000 geologic mapping (Minjárez Sosa *et al.* 2002; Ramírez Tello and Garcia Peralta 2004) and unpublished mining company reports, which recognized a red bed sequence in the region but did not describe the geologic setting of these rocks. The geologic mapping for this study was primarily centred on the village of Cerocahui and around Bahuichivo, and on the two main roads that transect the basin on the north and the east (Figures 2 and 3; Plate 1). Much of the central and southwestern sections of the basin are inaccessible due to lack of roads or hazards related to drug cultivation in the region; however, the geology located in these areas (noted on Figure 3) is interpreted from aerial imagery and based on known geologic relationships from the more accessible areas along the major roads and around population centres (Figure 2).

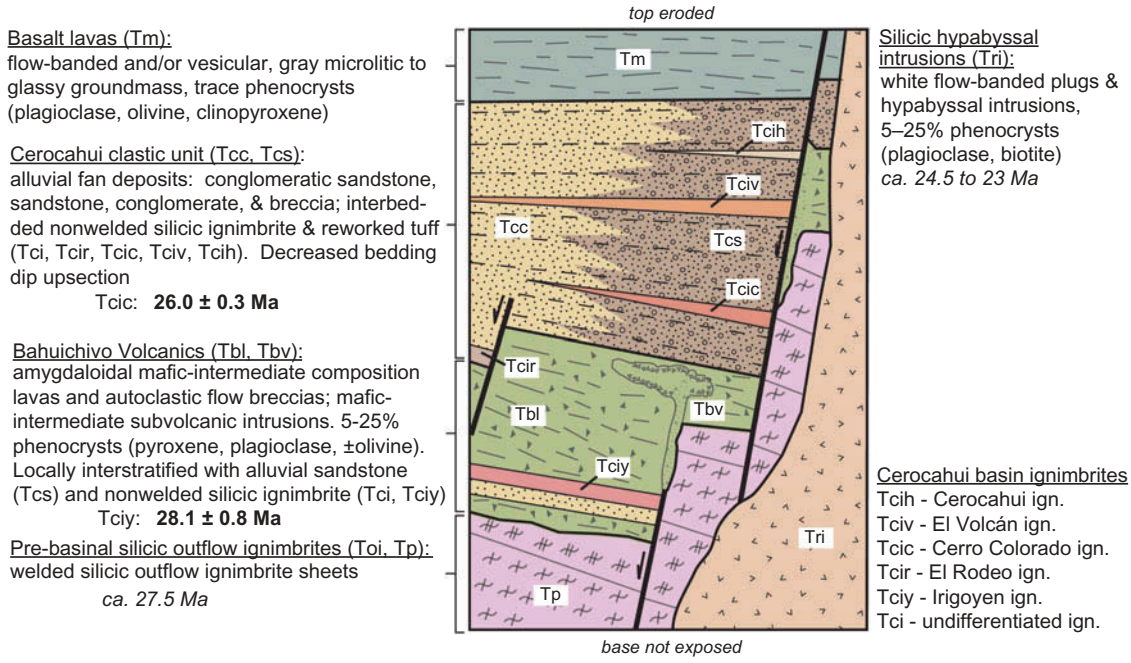

Figure 5. Rock units of the Cerocahui basin and substrate, depicting the characteristics and depositional relationships between the pre-basinal silicic outflow ignimbrites, Bahuichivo volcanics, Cerocahui clastic unit, basalt lavas, and silicic hypabyssal intrusions. Unit symbols are the same as in Figure 3. The ages in bold are from this study (Figure 10; Table 2), and the approximate ages in italics are from Murray *et al.* (2013) and are based on inferred stratigraphic correlations in the Guazapares Mining District to the west (see Figure 12; text for discussion).

NNW-trending normal faults are the primary geologic structures in the Cerocahui basin and the adjacent region (Figures 2–4; Plate 1). The W-dipping Bahuichivo–Bachamichi fault forms the eastern boundary of the Cerocahui basin. Immediately east (<1 km) and trending parallel to the Bahuichivo–Bachamichi fault is the W-dipping Pañales fault, which has a much thinner section of volcanic and sedimentary rocks on its hanging wall and lacks these rocks on its footwall; this fault thus represents a minor strand of the main basin-bounding fault (Figures 3 and 4A; Plate 1). Several W-dipping normal faults offset the deposits within the Cerocahui basin, including the Cerocahui, El Rodeo, and Irigoyen faults, but these have less offset than the eastern basin-bounding fault (Figures 3 and 4; Plate 1). Extension on these faults has gently to moderately tilted the strata of the Cerocahui basin to the north-to-northeast (~5–30°). The western boundary of the Cerocahui basin is inferred to be roughly in the location of the NW-trending, E-dipping Piedra Bola fault (Figures 2 and 3; Plate 1). This fault is younger than and offsets the lowermost deposits of the Cerocahui basin that extended westward onto the footwall block prior to fault motion (Figures 3 and 4A; Plate 1). Additionally, the basin fill on the hanging wall (east side) of the Piedra Bola fault dips away from the fault rather than toward it; therefore, the Piedra Bola fault is not considered a basin-bounding normal fault.

Basin stratigraphy and relation to extensional structures

The rocks exposed in the Cerocahui basin and surrounding area are subdivided into five lithologic units described in the following (from oldest to youngest): (1) pre-basinal silicic outflow ignimbrites, (2) the Bahuichivo volcanics, consisting mainly of mafic-intermediate composition lavas and subvolcanic intrusions, (3) the Cerocahui clastic unit, composed of alluvial fan sandstones, conglomerates, and breccias and interbedded silicic ignimbrites, (4) basalt lavas, and (5) silicic hypabyssal intrusions (Figures 3 and 5).

Silicic outflow ignimbrites of pre-basinal origin (Toi & Tp)

A section of tabular, largely welded silicic outflow ignimbrites is exposed in the footwall of the W-dipping Bahuichivo–Bachamichi and Pañales faults on the east side of the Cerocahui basin (map unit Toi) and in the footwall of the E-dipping Piedra Bola fault on the west side of the basin (Tp) (Figures 2 and 3). These two map units are tentatively correlated, although the ignimbrites east of the basin have not been studied in the same detail as those located west of the basin (Parajes Formation [Tp]) by Murray *et al.* (2013). At least seven distinct ignimbrites have been identified in the Parajes formation (Tp) on the west side of the Cerocahui basin; each ignimbrite ranges

from ~20 to ~210 m thick, has a densely welded to partially welded lower section that passes upward into a less-welded to non-welded top, and has normal coarse-tail grading of lithic fragments and inverse coarse-tail grading of pumice (Murray *et al.* 2013).

Because the silicic outflow ignimbrite section bounds the Cerocahui basin on both sides, and forms a widespread sheet where it has been mapped to the west and east (Figures 3 and 4), it is inferred to underlie the deposits of the Cerocahui basin. This interpretation is supported by an angular unconformity between gently dipping (~10° E) mafic-intermediate lavas (Tbl), fluvial sandstone, and an undifferentiated silicic ignimbrite (Tci) interpreted as part of the lowermost deposits of the Cerocahui basin (Bahuichivo volcanics, described below) and the underlying moderately dipping (~25° E) Parajes formation (Tp) on the western side (footwall) of the Piedra Bola fault near Irigoyen (Figures 3 and 4A; Plate 1). In the Guazapares Mining District region immediately west of the Cerocahui basin, normal faulting began during deposition of the youngest units in the Parajes formation (Tp) silicic outflow ignimbrite section after 27.6 ± 0.3 Ma (Murray *et al.* 2013). Map data in the silicic outflow ignimbrite section east of the Cerocahui basin are insufficient to determine whether any of the units are synextensional.

The silicic outflow ignimbrites on the east side of the Cerocahui basin are interpreted as the medial facies of outflow ignimbrite sheets, based on their sheet-like geometry and the presence of cliff-forming welded sections, similar to the ca. 27.5 Ma Parajes formation (Tp) to the west of the basin (Murray *et al.* 2013). Their sheet-like geometry is also similar to that of ignimbrites in the unextended core of the Sierra Madre Occidental, although that region also contains caldera-filling ignimbrites (e.g. Swanson *et al.* 2006). The silicic outflow ignimbrites on the east side of the Cerocahui basin (Toi) have not been dated directly, but they are clearly older than the basal basin-filling sedimentary deposits, and an intrusion of the Bahuichivo volcanics (Tbv) crosscuts one of the ignimbrites (Figure 6A). The ignimbrites generally have <15% phenocrysts and lack potassium feldspar (e.g. Swanson *et al.* 2006; Murray *et al.* 2013). Crystal-rich ignimbrites are rare and may prove correlatable by future workers; one such ignimbrite is located ~3.5 km southeast of Bahuichivo (Figure 3), with 30–35% phenocrysts of plagioclase, biotite (to 3 mm), quartz, hornblende, and 10% andesitic volcanic lithic lapilli.

Bahuichivo volcanics (Tbl & Tbv): lowermost Cerocahui basin fill

The stratigraphically lowest rocks considered part of the Cerocahui basin are the Bahuichivo volcanics, an informally named unit consisting of dark-coloured pyroxene-plagioclase- ± olivine-bearing amygdaloidal lavas and autoclastic flow breccias (Tbl), and similar lavas that are complexly intruded by dikes and subvolcanic intrusions (Tbv) (Figures 3–6). Based on the phenocryst assemblage (olivine, pyroxene, and plagioclase), these rocks suggest a mafic to intermediate composition.

Within the Cerocahui basin, the Bahuichivo volcanics are dominantly lavas, with individual flows up to ~20 m thick that dip moderately eastward (to ~20° E) toward the eastern basin-bounding faults (Figures 3 and 4). The base of the Bahuichivo volcanics is not exposed in the Cerocahui basin; the unit is the thickest (>500 m thick) in the southwestern mapped part of the basin and likely extends westward to the Piedra Bola fault based on aerial imagery. In the northwestern mapped part of the basin near Irigoyen (Figure, 3), lavas of the Bahuichivo volcanics (Tbl) are interstratified with alluvial red bed sandstones (Tcs) identical to those throughout the basin described below (Figures 3 and 4A), and locally wet sediment–lava intermixing (peperite) is present (Figure 6A). Also interbedded with the Bahuichivo volcanics in this area is the Irigoyen ignimbrite (Tciy), a light grey, crystal-poor, non-welded silicic ignimbrite with faint compaction foliation of slightly flattened white to tan pumice fragments. Based on this evidence, the lavas of the Bahuichivo volcanics are considered part of the Cerocahui basin fill.

The Bahuichivo volcanics are inferred to have erupted from fault-controlled volcanic centres along the eastern half-graben basin margin. Subvolcanic intrusions occur in the Bahuichivo area, where dikes and intrusions emplaced along small-offset NW-trending structures in the fault-block between the Pañales and Bahuichivo–Bachamichi faults complexly crosscut related lava flows (Tbv), as well as sandstones and conglomerates inferred to be related to the basin fill (Tcc and Tcs, described below) and pre-basinal silicic outflow ignimbrites (Toi) described above (Figures 3, 6B, and 6C; Plate 1). A mafic-intermediate dike that parallels the Irigoyen fault on the western side of the basin (Figures 3 and 6D) may have been an additional vent for the volcanic rocks (Tbl) located in this area. The localization of these shallow intrusions on NW-trending structures that trend parallel to the basin-bounding normal faults suggests that these structures provided a conduit for mafic to intermediate magmatism, and that extensional deformation occurred prior to and during emplacement of the Bahuichivo volcanics.

Cerocahui clastic unit (Tcc & Tcs): Cerocahui basin fill

The majority of the rocks in the Cerocahui basin are part of the over 700 m-thick Cerocahui clastic unit (Tcc and Tcs; Figures 3, 4, 5, 7, and 8). The rocks of the Cerocahui clastic unit are subdivided into eight sedimentary lithofacies (after Miall 1985; Uba *et al.* 2005; Murray *et al.* 2010) that allow for interpretations of depositional

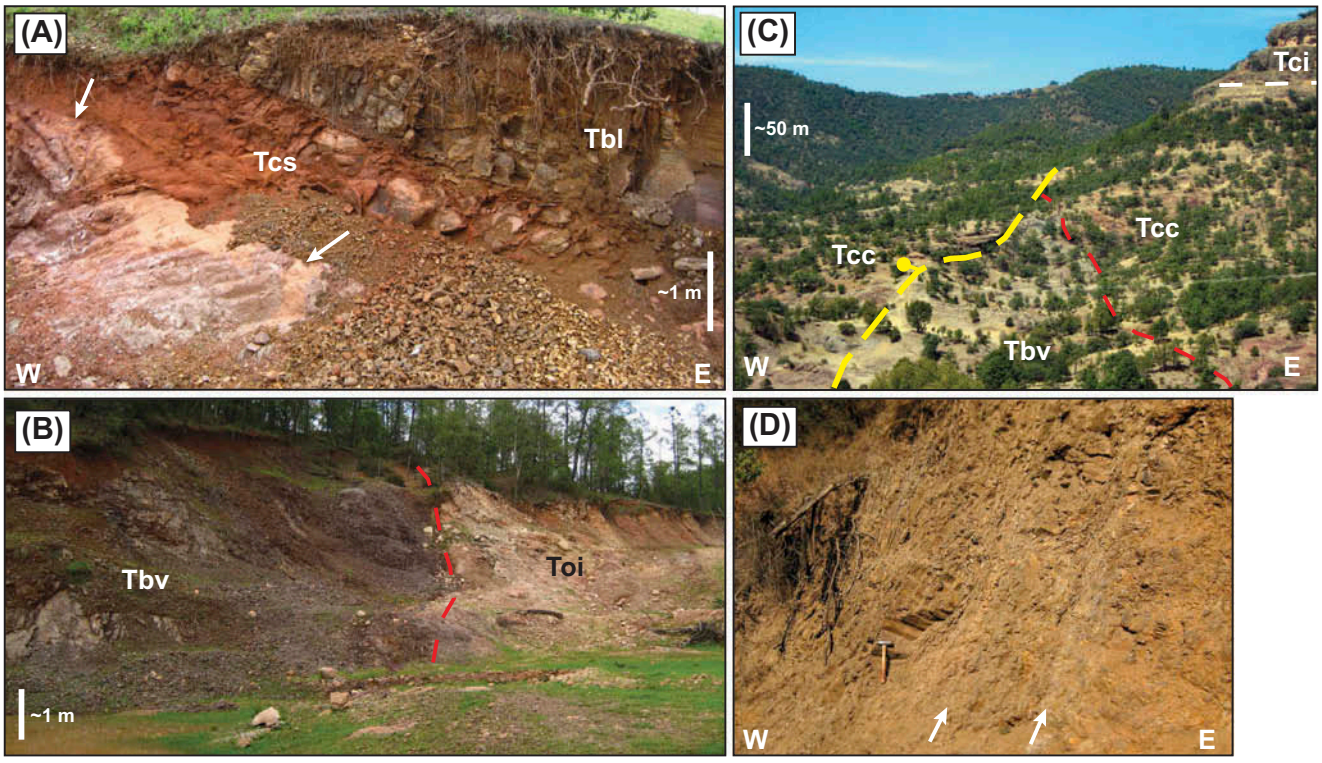

Figure 6. Representative photographs of the Bahuichivo volcanics; locations of the photographs are given (NAD27). (A) E-dipping mafic-intermediate lava (Tbl) deposited on massive red bed sandstone (Tcs) along the Bahuichivo–Irigoyen road (27.36320° N, 108.15692° W). Wet sediment–lava intermixing (peperitic texture) is found between the orange-tan sandstone (Tcs) and a lower reddish-grey mafic-intermediate lava (arrows). (B) Mafic-intermediate hypabyssal intrusion (Tbv) emplaced into lithic-rich pre-basinal non-welded silicic outflow ignimbrite (Toi) along the Bahuichivo–Cerocahui road (27.36228° N, 108.03371° W). (C) Mafic-intermediate hypabyssal intrusion (Tbv) emplaced into conglomerates and sandstones (Tcc) north of Bahuichivo (looking northwest from 27.42259° N, 108.07175° W). Intrusion and sedimentary rocks are offset by the Bahuichivo–Bachamichi fault (yellow dashed line, tick mark on the hanging wall). Cliff of silicic ignimbrite (Tci) deposited over Tcc is ~50 m tall. (D) W-dipping mafic-intermediate composition dike exhibiting columnar jointing emplaced along a small-scale structure that trends sub-parallel to the Irigoyen fault, along the Bahuichivo–Irigoyen road (27.36493° N, 108.14926° W). Small-offset faults related to the Irigoyen fault (arrows) cut lavas of the Bahuichivo volcanics to the right of the dike.

processes (Table 1). This unit consists of volcaniclastic sandstones, conglomerates, and breccias, with interbedded non-welded silicic ignimbrites and fluvially reworked tuffs (Figures 5, 7, and 8), deposited in angular unconformity over the mafic-intermediate lavas of the Bahuichivo volcanics (Figures 3 and 4). All of the deposits of this stratigraphic unit thicken and coarsen eastward toward the basin-bounding normal faults, with conglomerates and breccias (lithofacies Gm and Gc; Table 1) restricted to the area adjacent to the Bahuichivo–Bachamichi fault (Figures 3, 4, and 8A–8D). The bulk of the deposits in the Cerocahui clastic unit consist of medium to very thickly bedded, moderately to very poorly sorted, medium-to-very coarse-grained volcaniclastic sandstones and conglomeratic sandstones (lithofacies Sm; Table 1; Figures 5, 7, and 8B). The conglomeratic sandstones are composed of <30% gravel-sized (>2 mm, to 0.5 m diameter) subrounded to subangular clasts derived from amygdaloidal mafic-intermediate lavas, silicic flow-banded lavas, and silicic welded to non-welded ignimbrites. Intercalated with the conglomeratic sandstones on the eastern margin of the basin are medium to very thickly bedded matrix-supported granule to boulder (to 1 m diameter) angular-to-subrounded conglomerates and breccias (lithofacies Gc and Gm; Table 1), which have similar clast compositions to the conglomeratic sandstones (Figures 7 and 8B–8D). The rocks of this unit contain sedimentary structures indicative of fluvial deposition, including channels that indicate southwestward-directed palaeoflow, cut-and-fill structures, trough and low-angle cross-stratification (lithofacies Sx; Table 1), and normal to inverse graded bedding (Figures 7, 8B, and 8D–8G).

Silicic non-welded ignimbrites and fluvially reworked tuff (tuffaceous sandstones and conglomerates, lithofacies Vr; Table 1) are interbedded within the Cerocahui clastic unit, with four distinct and informally named ignimbrites recognized: the El Rodeo, Cerro Colorado, El Volcán, and Cerocahui ignimbrites (Figures 3, 4, 7, 8A, 8F–8I;

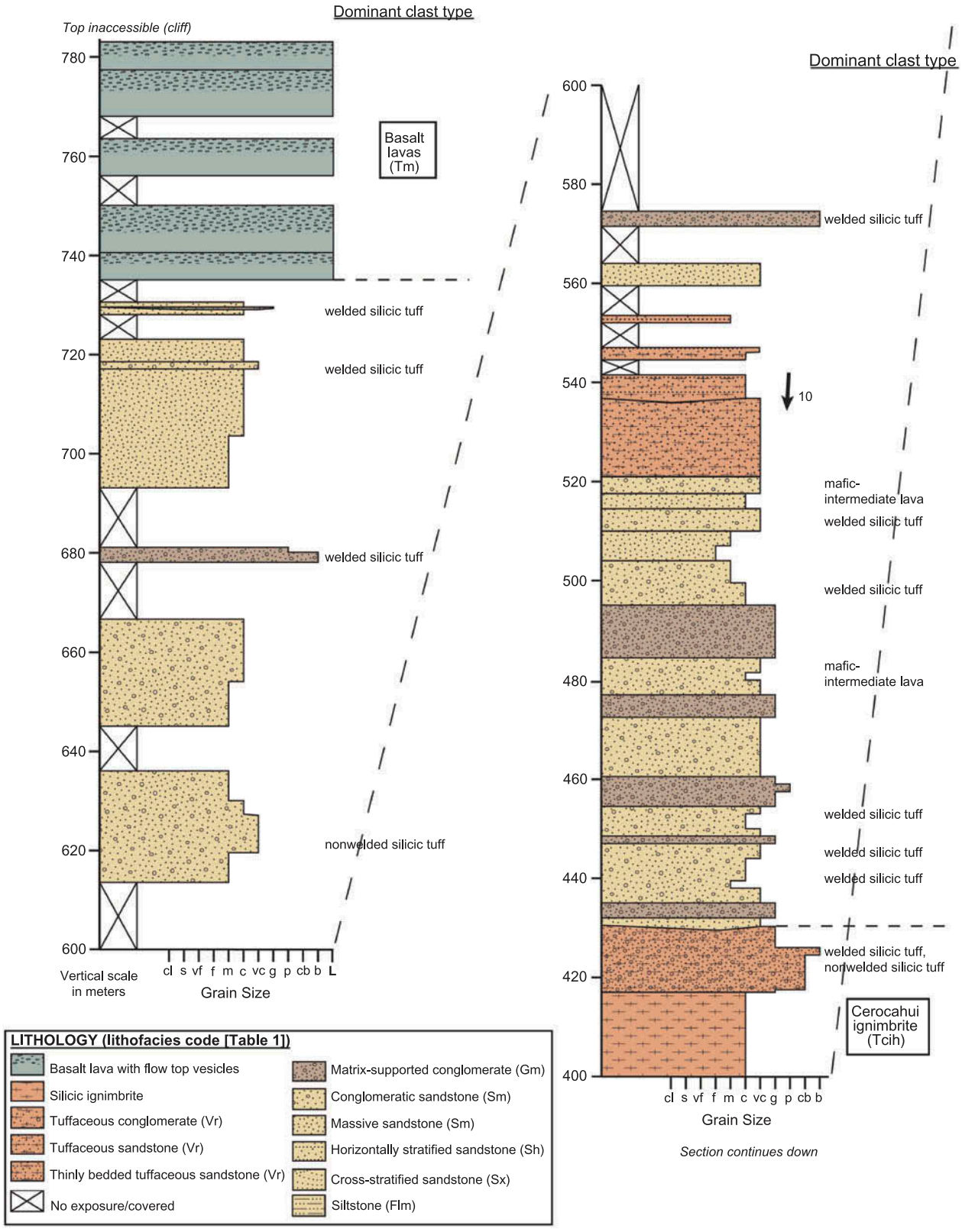

Figure 7. Measured stratigraphic section of the Cerocahui clastic unit (map unit Tcc) through basalt lavas (Tm) in the Cerocahui village area (see Figure 3), including facies types (Table 1), palaeocurrent data from trough limbs (method I of DeCelles *et al.* 1983), and the dominant clast composition of conglomerates and conglomeratic sandstones, is listed where recorded in the section. The three informally named non-welded silicic ignimbrites interbedded within the Cerocahui clastic unit and the stratigraphic position of U-Pb sample BM080718–1 (Figure 10; Table 2) are also indicated. Lithofacies associations suggest that this stratigraphic section represents medial-proximal alluvial fan deposits in the Cerocahui basin.

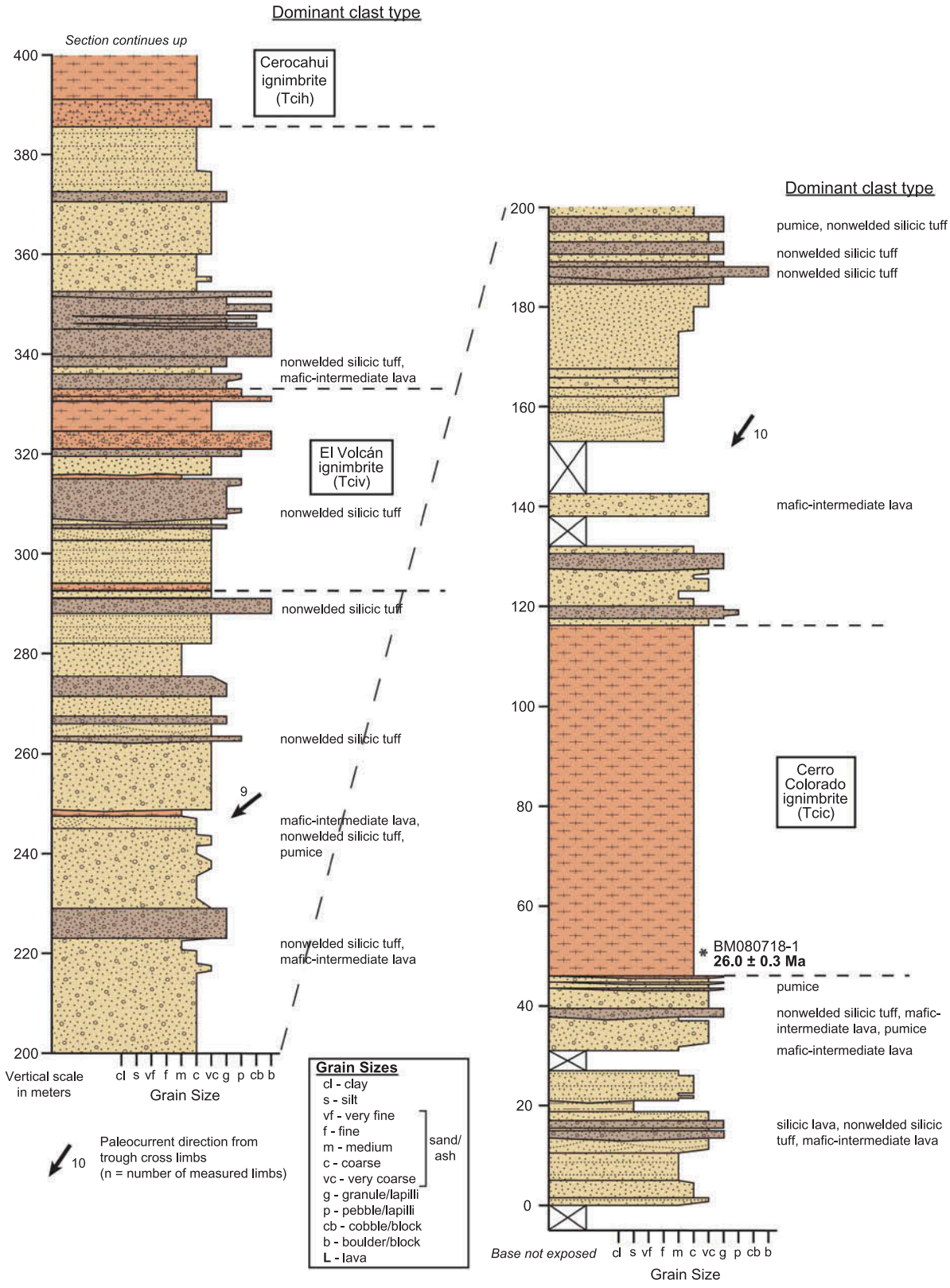

Figure 7. (Continued)

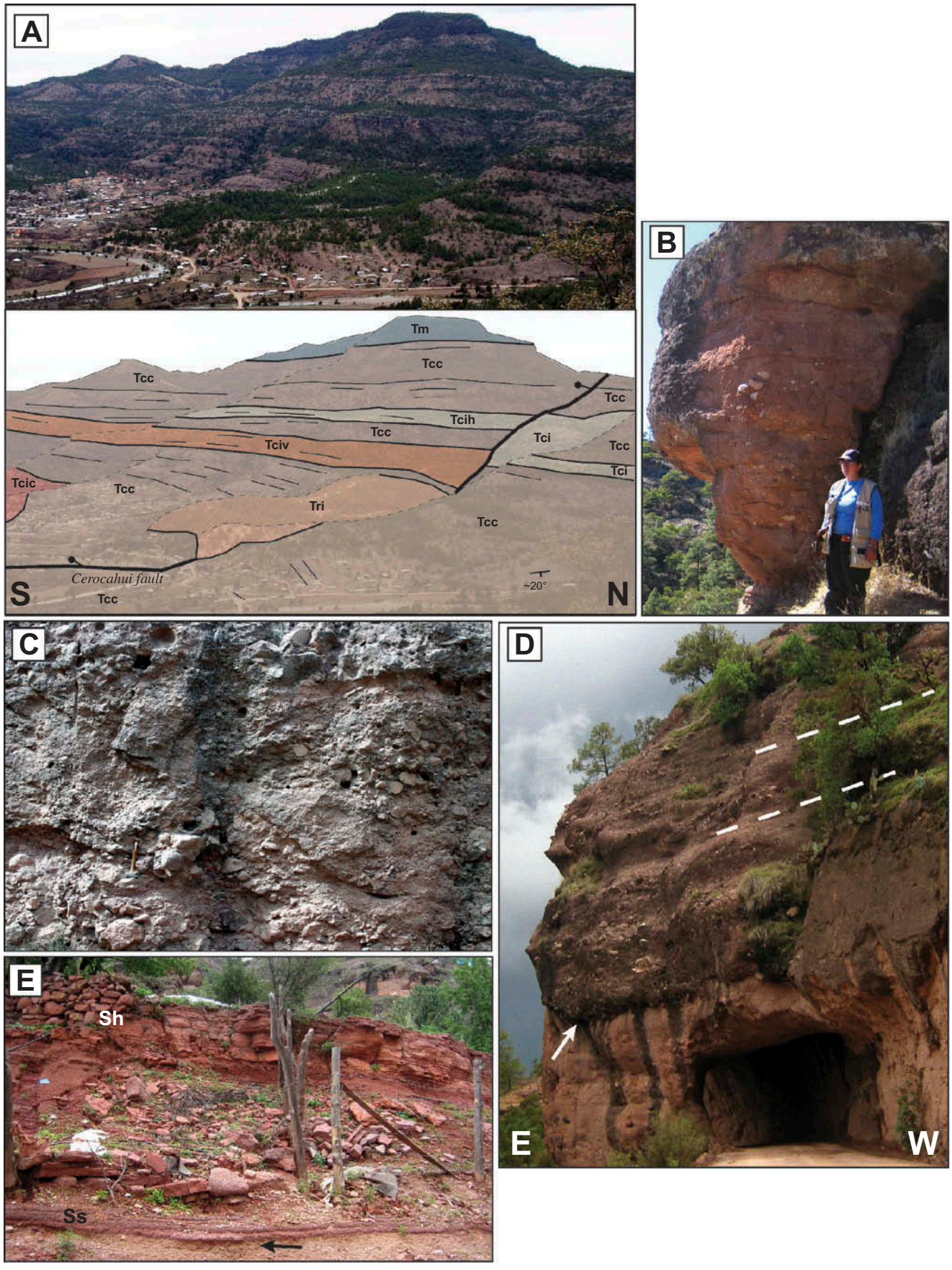

Figure 8. Representative photographs of the Cerocahui clastic unit and interbedded silicic ignimbrites; locations of photos are given (NAD27). (A) Overview photograph and geologic interpretation of the Cerocahui basin (looking west from 27.29390° N, 108.03736° W),

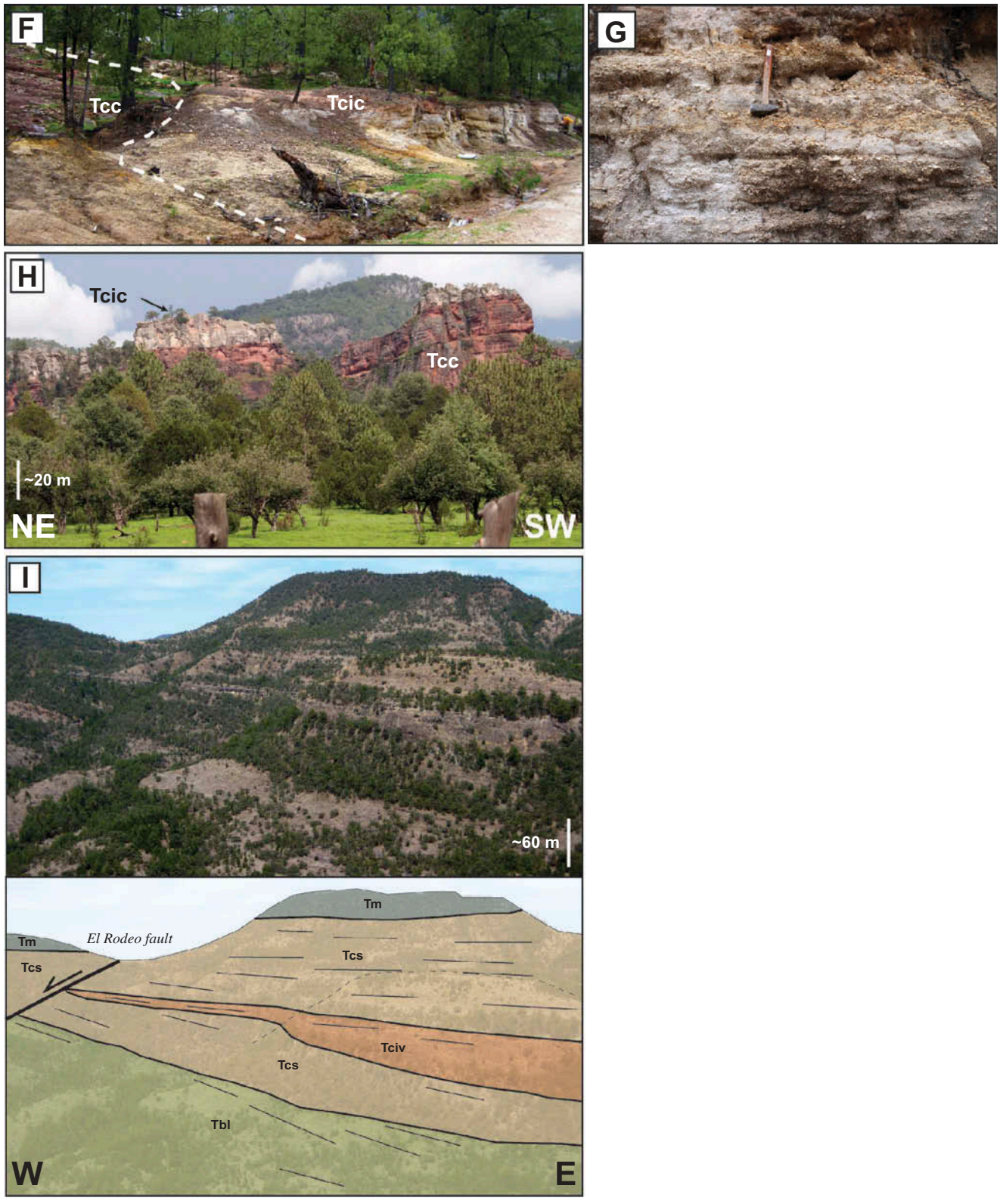

Figure 8. (Continued)
showing moderately E-dipping (to ~15° NE) Cerocahui clastic unit (Tcc) below gently N-dipping to sub-horizontal Cerro Colorado ignimbrite (Tcic), Cerocahui clastic unit, El Volcán ignimbrite (Tciv), Cerocahui ignimbrite (Tcih), and undifferentiated silicic ignimbrite (Tci), with basalt lavas (Tm) conformably deposited over the Cerocahui clastic unit. The N-trending Cerocahui fault (tick marks on hanging wall) downdrops the Cerocahui clastic unit to the west, with a silicic hypabyssal intrusion (Tri) emplaced along the fault and crosscutting it. (B) Massive (~4 m thick) matrix-supported conglomerate (lithofacies Gm; Table 1) with weak inverse grading (left of person) interbedded within conglomeratic sandstone at 225 m on measured stratigraphic section (Figure 7). Clasts consist of subangular reddish-grey mafic-intermediate volcanic and white non-welded silicic ignimbrite fragments (27.30315° N, 108.06420° W). (C) Clast-

Table 1. Sedimentary lithofacies of the Cerocahui clastic unit*.

Facies code	Description	Interpretation
Gc	Clast-supported, massive conglomerate and breccia. Dark red to grey. Very poorly sorted, angular to subrounded. Pebbles to boulders with fine-to-very coarse-grained sand matrix. Thickly to very thickly bedded, lobate to tabular bedding extending laterally for several metres to a few hundred metres. No to very poorly developed normal to inverse grading.	Clast-rich debris flow deposits, rapid deposition by stream-floods with concentrated clasts
Gm	Matrix-supported, massive conglomerate. Dark red to grey. Very poorly sorted, subangular to subrounded. Granules to boulders in medium-to-very coarse-grained sand matrix. Medium to very thickly bedded, lenticular to tabular bedding extending laterally for several metres to several hundred metres. No to very poorly developed normal to inverse grading.	Plastic debris flow deposits, deposited from hyperconcentrated or turbulent flow
Sm	Massive sandstone. Tan to red. Medium-to-very coarse-grained, locally conglomeratic with <30% subrounded to subangular pebbles to boulders. Moderately to very poorly sorted. Medium to very thickly bedded, lenticular to tabular bedding extending laterally for tens of metres to a several hundred metres. No to very poorly developed normal to inverse grading.	Hyperconcentrated sediment-gravity flows, rapid deposition
Sx	Cross-stratified sandstone. Tan to red. Trough and low- angle (<10°) cross-stratification. Fine-to-very coarse-grained. Thinly to thickly bedded, lenticular bedding extending laterally for tens of metres, trace lenses of granule to pebbles. Moderately to well sorted.	Channel fills, crevasse splays, dune migration
Sh	Horizontally stratified sandstone. Tan to red. Very fine-to- coarse-grained, trace lenses of cobbles and pebbles. Well to moderately sorted. Very thinly to thickly bedded, tabular bedding extending laterally for several tens of metres to a few hundred metres.	Planar bed flow, upper flow regime
Ss	Sandstone with basal scour surface. Red to tan. Very coarse-to-medium-grained, locally conglomeratic with <30% granules to pebbles. Normal grading. Lenticular, extending laterally for several metres.	Erosive channel fills
Flm	Massive or laminated siltstone. Red. Lenticular to tabular bedding, extending laterally for tens of metres.	Overbank, abandoned channel or suspension deposits
Vr	Tuffaceous sandstone or conglomerate. White to light tan. Medium-to-very coarse-grained sand, granules to boulders. Subangular to subrounded pumice fragments. Laminated to thickly bedded, lenticular to tabular bedding extending laterally for less than one metre to tens of metres. Moderately to poorly sorted.	Reworked primary silicic tuff

Note: *After Miall (1985), Uba *et al.* (2005), and Murray *et al.* (2010).

Plate 1). Of these four ignimbrites, the El Rodeo ignimbrite (Tcir) is the stratigraphically lowest. Exposures of this ignimbrite are restricted to the west side (hanging wall) of the El Rodeo fault (described below), where it is deposited directly on the underlying mafic-intermediate lavas of the Bahuichivo volcanics (Figures 3 and 4B). The El Rodeo ignimbrite is non-welded with a tan to light pink groundmass, 20% phenocrysts of plagioclase,

supported conglomerate-breccia (lithofacies Gc; Table 1) with mafic-intermediate volcanic boulders to ~1 m in a medium-to-very coarse-grained sand matrix, interpreted as proximal alluvial fan debris flow deposits adjacent to the Bahuichivo–Bachamichi fault along the Bahuichivo–Cerocahui road (27.34576° N, 108.03776° W). (D) E-dipping matrix-supported conglomerate (lithofacies Gm; Table 1) cutting and filling a channel (arrow) in underlying conglomeratic sandstone (lithofacies Sm; Table 1) adjacent to the Bahuichivo–Bachamichi fault northeast of Cerocahui (27.30809° N, 108.04059° W). (E) Horizontally stratified fine-to-medium-grained sandstone (lithofacies Sh, Ss; Table 1), with a small-scale cut-and-fill structure (arrow; ~10 cm deep) (27.30210° N, 108.06152° W). (F) Reworked pumice lapilli-tuff at the base of the Cerro Colorado ignimbrite (Tcic), infilling a ~4 m deep channel cut into underlying conglomeratic sandstone (Tcc); close-up of this pumice lapilli-tuff shown in Figure 8G (27.29829° N, 108.06447° W). (G) Close-up of basal reworked pumice lapilli-tuff (lithofacies Vr; Table 1) of the Cerro Colorado ignimbrite (Figure 8F), with well-sorted lenses of granule to pebble subangular pumice (tan) interbedded within grey tuff (27.29829° N, 108.06447° W). (H) View looking southeast from near base of the measured stratigraphic section (Figure 3; 27.29358° N, 108.06592° W) at Cerro Colorado, with N-dipping white Cerro Colorado ignimbrite (Tcic) capping hill, above red Cerocahui clastic unit (Tcc). (I) Overview photograph and geologic interpretation of growth strata east of the El Rodeo fault in the south-central section of the Cerocahui basin (Figure 3), looking north from Cerro El Volcán (27.31205 ° N, 108.09606° W). The dip of the units changes from ~20° E in the lowermost mafic-intermediate lavas (Tbl), through 10° to 5° within the Cerocahui clastic-unit (Tcs), to ~0° in the capping basalt lavas (Tm), and the unit thicknesses of the Cerocahui clastic unit (Tcs) and El Volcán ignimbrite (Tciv) also increase eastward, indicating syndepositional extension of the eastern fault-bounded margin of the Cerocahui basin. Similar depositional relationships are found on the hanging wall of the El Rodeo fault (Figure 4B), suggesting syndepositional extension of this fault, with continued postdepositional extension that downdropped the basalt lavas (Tm) to the west.

biotite, and hornblende, trace lithic fragments, and 25% yellow and salmon-coloured pumice fragments. The Cerro Colorado ignimbrite (Tcic) crops out in the low-lying areas near Cerocahui and caps Cerro Colorado to the south of the village (Figures 3, 8A, and 8H). The Cerro Colorado ignimbrite is at least 70 m thick (Figure 7), has a light tan groundmass near the base that transitions to light grey at the top, ~5% phenocrysts of plagioclase (to 1.5 mm) and biotite (<1 mm), trace white long-tube pumice fragments (to 2 cm), and trace mafic-intermediate volcanic lithic fragments (to 5 mm). The base of the Cerro Colorado ignimbrite locally consists of a reworked pumice lapilli-tuff deposit (lithofacies Vr; Table 1) that infills a ~4 m-deep channel cut into underlying sandstone (Figure 8F–8G). The El Volcán ignimbrite (Tciv) forms part of a prominent ~80 m cliff in the middle part of the ridge north of Cerocahui and extends westward for ~6.5 km, pinching out north of El Rodeo (Figures 3, 7, 8A, and 8I; Plate 1). The western deposits of this ignimbrite located at Cerro El Volcán have limited reworking and no interbedded sedimentary deposits and consist of several thin (<5 m thick) non-welded primary outflow sheets with a tan to white groundmass, 10–20% phenocrysts (<1 mm) of plagioclase, biotite, and trace clinopyroxene, hornblende, and quartz, <5% lithic fragments (<1 mm), and 15–30% white to yellow long-tube pumice fragments (to 10 mm). At the location of the measured stratigraphic section northwest of Cerocahui, closer to the eastern basin margin, the El Volcán ignimbrite is predominantly fluvially reworked and interbedded with conglomerates and sandstones (Figure 7; 292–332 m above the section base). The Cerocahui ignimbrite (Tcih) is a ~27 m-thick unit that crops out on the ridge north of Cerocahui (Figure 3, 7, and 8A). This ignimbrite is non-welded with a white groundmass, 10–15% phenocrysts of plagioclase, biotite, quartz, and hornblende, 5–10% lithic fragments (~1 mm), and 15% yellow pumice fragments. The base and top of the Cerocahui ignimbrite consist of reworked lapilli-tuff (tuffaceous sandstone and conglomerate) that is similar in composition to the primary ignimbrite, but is more stratified and better sorted than the rest of the ignimbrite deposit (Figure 7).

Based on stratigraphic relations and sedimentary lithofacies (Table 1), the Cerocahui clastic unit likely represents deposition in alluvial fan systems (e.g. Miall 1985; Kelly and Olsen 1993; Blair and McPherson 1994; Collinson 1996; Murray *et al.* 2010). The interpretation of these sedimentary rocks as alluvial deposits is supported by the presence of clast-to-matrix-supported conglomerates, breccias (lithofacies Gc and Gm; Table 1), and conglomeratic sandstones (lithofacies Sm; Table 1) interpreted as sediment-gravity flow deposits, stratified to cross-stratified sandstones (lithofacies Sh and Sx; Table 1) interpreted as fluvial deposits, and deposits that infill channels cut into underlying strata (Figures 7 and 8B–8G). The silicic ignimbrites interstratified with the volcaniclastic rocks were likely erupted from distal sources and deposited in the basin, based on their non-welded nature and high proportion of interstratified fluvially reworked tuff (Figure 7).

Deposition of the Cerocahui clastic unit likely occurred during extensional deformation of the eastern basin-bounding normal faults. Evidence of synextensional deposition includes the increased thickness and coarseness of the Cerocahui clastic unit toward the basin-bounding fault, with these deposits either ending at the Bahuichivo–Bachamichi fault or thinning onto the fault-block between the Bahuichivo–Bachamichi and Pañales faults (Figures 3 and 4; Plate 1). Evidence of possible growth strata is indicated by an upsection decrease in bedding dip from ~18° E to 6° E observed within the Cerocahui clastic unit along the Irigoyen–Bahuichivo road, as well as an upsection dip decrease from 13° E to 5° N in the vicinity of the measured stratigraphic section near Cerocahui (Figures 3 and 4; Plate 1). The more northerly bedding dips in the Cerocahui area may represent the slightly tilted original orientation of the alluvial fan deposits, or they may reflect greater fault activity and subsidence in the northern part of the basin, either on the basin-bounding faults or on unmapped intra-basinal faults, which tilted the rocks in that direction. In addition, angular unconformities between and within the Bahuichivo volcanics, Cerocahui clastic unit, and basalt lavas (described below) are observed within the basin (Figures 3, 4, 8A, and 8I; Plate 1). These unconformities and upsection changes in bedding dip angle can be explained either by the crustal flexural subsidence related to sediment loading or by the syndepositional tilting related to normal fault motion on the eastern half-graben margin (i.e. growth strata). The latter explanation of synextensional deposition is preferred, given the limited, thinner exposures of Cerocahui basin deposits east of the Bahuichivo–Bachamichi fault and the sub-parallel NW-alignment of Bahuichivo volcanic intrusions to the half-graben bound fault system.

Syndepositional extension of the El Rodeo fault within the basin is suggested by the restriction of the El Rodeo ignimbrite (Tcir) to the hanging wall of this fault, gently dipping (<5° E) Cerocahui clastic unit rocks deposited in angular unconformity above moderately tilted (15° E) Cerocahui clastic unit sandstone on the hanging wall of the fault, and greater vertical fault offset of the El Volcán ignimbrite (Tciv; ~125 m-vertical offset) compared to the overlying basalt lavas (described below; ~100 m-vertical offset) (Figures 4B and 8I; Plate 1). Additional syndepositional to postdepositional offset of the Bahuichivo–Bachamichi and El Rodeo faults resulted in the development of drag synclines on the hanging wall adjacent to these faults (Figures 3 and 4B; Plate 1).

Basalt lavas: uppermost Cerocahui basin fill

Conformably overlying the Cerocahui clastic unit is a flat-lying to gently dipping (<5°) basalt lava unit (Tm; Figures 3, 4, 7, and 8A; Plate 1). The basalt lavas are widespread and appear to cap all of the ridges within the study area (Figure 3; Plate 1). This unit is composed of several lavas that have flow-banded interiors and vesicular flow tops, with individual flows to ~10 m thick (Figure 7). These basalt lavas are grey with a microlitic to glassy groundmass, and contain trace phenocrysts of plagioclase, olivine, and clinopyroxene. The entire stratigraphic unit has an estimated thickness of over 300 m, with the greatest thickness in the northwestern part of the basin (Figure 3; Plate 1). The vents for the basalt lava flows have not been identified within the study area.

The basalts appear to have been erupted just prior to the end of extensional deformation in the basin, because the stratigraphic unit is vertically offset across the El Rodeo fault and the Bahuichivo–Bachamichi fault north of Bahuichivo, and is not present on the footwall of the Pañales fault (Figure 4A). The general flat-lying orientation of the basalt lavas and the slight amount of offset of this unit across the Bahuichivo–Bachamichi fault (<50 m vertical offset) suggest that extensional deformation in the basin was limited following eruption of this unit.

Silicic hypabyssal intrusions: post-basinal magmatism

The youngest lithologic unit in the study area is composed of silicic hypabyssal intrusions/plugs (Tri) that were emplaced following volcaniclastic and volcanic deposition in the Cerocahui basin (Figures 3, 5, 8A, and 9). These subvertically flow-banded intrusions are located along the southern mapped section of the basin-bounding Bahuichivo–Bachamichi fault (Figure 9A) and within the Cerocahui clastic unit along the Cerocahui fault where this fault that cuts the Cerocahui clastic unit diverges into two branches in the village of Cerocahui (Figures 3 and 8A). Although there are no direct crosscutting relationships, the silicic hypabyssal intrusions are inferred to be younger than the basalt lavas; this relative age relationship is based on the undeformed nature of the silicic intrusions and that they are emplaced along the southern projection of the basin-bounding fault near Cerocahui, which offsets the basalt lavas to the north near Bahuichivo (Figure 3; Plate 1), as well as along faults within the basin that offset older deposits of the Cerocahui clastic unit. Increased tilting of the Cerocahui clastic unit occurred adjacent to the margins of the intrusions during emplacement (Plate 1). The silicic hypabyssal intrusion near Cerocahui has a perimeter of flow-banded blocks (Figure 9B), suggesting brecciation during emplacement. The rocks of this intrusion are white, flow-banded, with 5–25% euhedral phenocrysts of plagioclase and biotite. Extrusive rocks associated with these silicic intrusions have not been identified in the Cerocahui basin area.

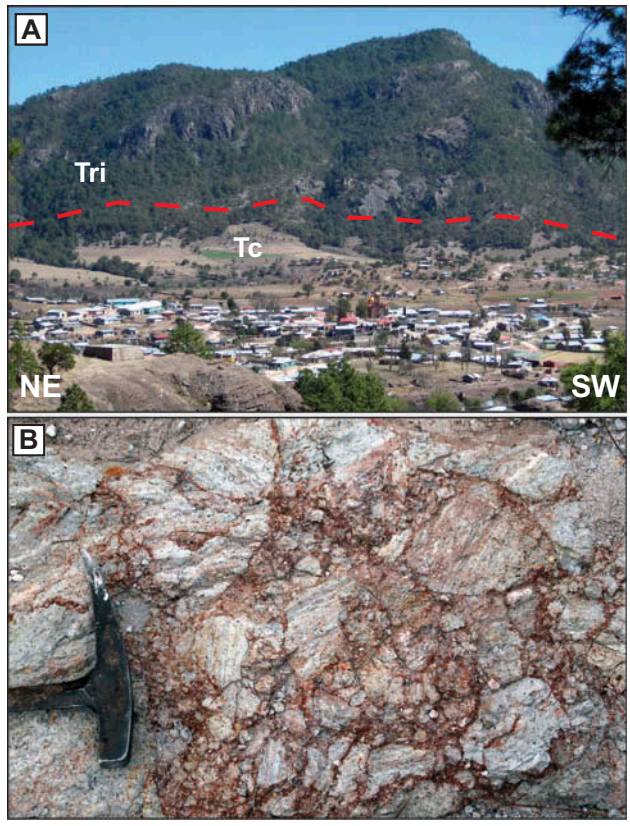

Figure 9. Representative photographs of the silicic hypabyssal intrusions (Tri); locations of photographs are given (NAD27). (A) Subvertically flow-banded intrusions emplaced into Cerocahui basin deposits (foreground) and forming a prominent ridge southeast of Cerocahui (centre), along the southern projection Bahuichivo–Bachamichi fault (Figure 3; looking southeast from 27.30569° N, 108.06423° W). (B) Flow-banded blocks in the brecciated perimeter of the silicic hypabyssal intrusion intruded along the Cerocahui fault (27.30202 ° N, 108.05304° W).

Depositional age constraints

Methodology & age interpretations

New U-Pb zircon ages were obtained from two silicic ignimbrites within the Cerocahui basin, providing constraints on the age of these previously undated deposits. Laser ablation inductively coupled plasma mass spectrometry (LA–ICP-MS) U-Pb analyses were performed at the Laboratorio de Estudios Isotópicos, Centro de Geociencias, Universidad Nacional Autónoma de México (UNAM), on zircons separated from the two silicic ignimbrite samples (Figure 10; Table 2), using the analytical methods and age calculations detailed in Murray *et al.* (2013). Concordia plots, probability density distribution

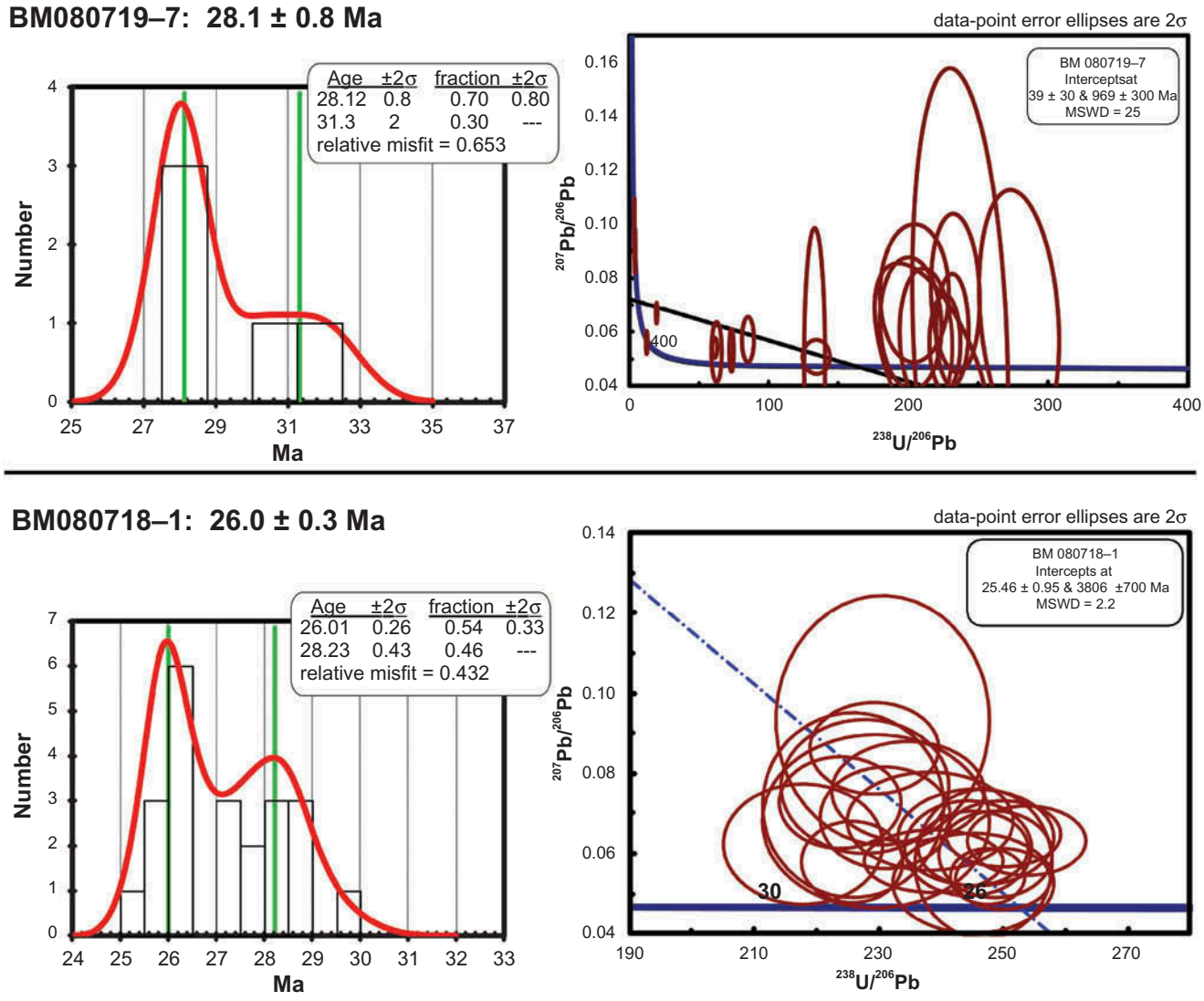

Figure 10. Summary of zircon U-Pb LA–ICP–MS analyses for samples listed in Table 2, with mean $^{206}Pb/^{238}U$ ages of the youngest zircon population (interpreted emplacement age) for each sample being listed. For each sample, probability density distribution plots with age calculations (left) using the deconvolution method in Isoplot 3.70 (Ludwig 2008) and Tera-Wasserburg concordia plots (right) are shown. MSWD, mean square of weighted deviates of initial zircon ages. Note that the vertical and horizontal scales of the probability density distribution plots differ between each sample. Details on the experiments are given in Supplemental Table 1.

Table 2. Summary of zircon U-Pb LA-ICP-MS results.

Sample	Map unit	Lithology	Age (Ma)*	±2σ (Ma)	n	Latitude (°N)	Longitude (°W)
BM080718–1	Tcic	Cerro Colorado ignimbrite	26.0	0.3	12	27.29832	108.06507
			28.2	*0.4*	10		
BM080719–7	Tciy	Irigoyen ignimbrite	28.1	0.8	3	27.36548	108.15269
			31.3	*2*	2		

Notes: LA-ICP-MS, laser ablation inductively coupled plasma mass spectrometry. Ages in italics represent the inherited zircon age population in a given sample (crystals that predate crystallization and eruption of a host magma). The youngest age population of each sample is interpreted as the phenocryst crystallization age and the maximum eruption age. Details of each analysis are given in Supplemental Table 1. North American Datum 1927 (NAD27) datum is used for latitude and longitude. Map unit labels correspond to Figure 3. The relative stratigraphic position of ages is shown in Figure 5. Locations of the samples are shown in Figures 3 and 7 and Plate 1. n, number of zircons used for age calculation.
*Mean $^{206}Pb/^{238}U$ age calculated using the deconvolution method in Isoplot 3.70 (Ludwig 2008).

and histogram plots, mean age, and age-error calculations were performed using Isoplot v. 3.70 (Ludwig 2008).

In the Sierra Madre Occidental, which has a long-lived 15–20 million year history of continuous magmatism, it is common to observe mixed-age populations due to zircon inheritance signatures. This is problematic for dating the younger (early Miocene) rocks, which often contain 'antecrysts', zircons that formed during earlier phases of related magmatism within the igneous province but are not directly crystallized from the host magma (e.g. Bryan *et al.* 2008; Ferrari *et al.* 2013; Murray *et al.* 2013). Where mixed-age populations are suggested (e.g. mean $^{206}Pb/^{238}U$ ages that yield MSWD [mean square of weighted deviates] values much greater than unity, probability density function curves that are positively skewed and asymmetric, and/or have broad, bimodal, or polymodal peaks), the deconvolution method, based on the mixture modelling method of Sambridge and Compston (1994), was implemented in Isoplot. In our analyses, we interpret the oldest zircon age population calculated using this method that is less than ca. 38 Ma in a sample represents the crystallization age of antecrysts incorporated into the host magma and that the youngest zircon age population indicates the age of phenocryst crystallization (after Ferrari *et al.* 2013), which we interpret as the maximum possible eruption age of the rock. Age results are presented in the following and summarized in Figure 10 and Table 2, with the locations of the samples shown in Figure 3 and Plate 1; detailed analytical data are given in Supplemental Table 1 (see http://dx.doi.org/10.1080/00206814.2014.941022).

Results

Sample BM080719–7 is from the Irigoyen ignimbrite (Tciy) at the northwestern basin margin near Irigoyen (Figures 3, 4A, and 5). This ignimbrite (described above) is interstratified with lavas of the Bahuichivo volcanics (Tbl) and the lowermost sandstones (Tcc) of the Cerocahui basin (Figures 3 & 4A; Plate 1). U-Pb data for this sample reveal the presence of several xenocrysts with Proterozoic (ca. 1.7 Ga; n = 1), Palaeozoic (ca. 481 and 318 Ma; n = 2), Late Cretaceous (ca. 104–75 Ma; n = 4), and early Eocene (ca. 48 Ma; n = 2) ages (Supplemental Table 1). From the analysis of five non-xenocrystic zircons (Figure 10; Table 2; Supplemental Table 1), two main zircon age populations are recognized in sample BM080719–7 consisting of an older grouping having a mean age of 31.3 ± 2 Ma and a younger grouping with a mean age of 28.1 ± 0.8 Ma (Figure 10; Table 2). The zircons of the older age population are likely antecrysts, while the zircons from the younger age population are interpreted as phenocrysts. The phenocryst age overlaps within uncertainty with ages of the pre-basinal silicic outflow ignimbrites to the west (e.g. 27.6 ± 0.3 Ma Puerto Blanco ignimbrite of the Parajes formation; Murray *et al.* 2013). Given the stratigraphic constraints and the large age uncertainties with sample BM080719–7 due to the limited number of analysed non-xenocrystic zircons, the Irigoyen ignimbrite (Tciy) is likely equivalent-age or slightly younger than the underlying Puerto Blanco ignimbrite, with an eruption age (based on uncertainties) between ca. 27.9 and 27.3 Ma. This age suggests that initial eruption of the Bahuichivo volcanics within the Cerocahui basin occurred ca. 27.5 Ma.

Sample BM080718–1 is from the base of the Cerro Colorado ignimbrite (Tcic; described above) near Cerocahui, which is interbedded in the lower section of the Cerocahui clastic unit stratigraphically above the Bahuichivo volcanics (Figures 3, 4B, 5, and 7). Unlike the previous sample, xenocrysts were not found in this sample. From the analysis of 22 zircons (Table 2; Supplemental Table 1), two age populations are recognized in sample BM080718–1, consisting of an older group with a mean age of 28.2 ± 0.4 Ma and a younger group that has a mean age of 26.0 ± 0.3 Ma (Figure 10; Table 2). Similar to the sample above, the older zircon age population is likely antecrystic, and the population of younger zircons is interpreted as phenocrysts. This phenocryst age overlaps within uncertainty with the age of the Témoris Formation in the Guazapares Mining District region, which is bracketed at ca. 27–24.5 Ma by U-Pb zircon ages of the underlying and overlying formations (Parajes and Sierra Guazapares formations, respectively) and interbedded silicic ignimbrites (Murray *et al.* 2013). In addition, this data provides a minimum age for the eruption of the underlying Bahuichivo volcanics at ca. 26 Ma.

Discussion

Cerocahui basin evolution

The new geologic mapping, stratigraphy, and geochronology presented in this study show that the rocks of the Cerocahui basin region record late Oligocene (ca. 27.5 Ma to likely older than 24.5 Ma) synextensional volcanism and volcaniclastic alluvial deposition during the mid-Cenozoic ignimbrite flare-up in the northern Sierra Madre Occidental. The developmental history of the Cerocahui basin includes (Figure 11): (1) deposition of welded silicic outflow ignimbrite sheets; (2) synextensional magmatism and deposition of the Bahuichivo volcanics, Cerocahui clastic unit, and basalt lavas in the Cerocahui basin during a lull in silicic ignimbrite flare-up volcanism; and (3) emplacement of silicic hypabyssal intrusions along pre-existing extensional faults in the Cerocahui basin.

The silicic outflow ignimbrite sheets that underlie the Cerocahui basin are similar to late Oligocene outflow ignimbrite sheets in adjacent regions of the northern Sierra Madre Occidental, which erupted during the end of the early Oligocene pulse of the ignimbrite flare-up (Swanson *et al.* 2006; Murray *et al.* 2013). Similar to the

ignimbrites of the Parajes formation in the Guazapares Mining District region (Murray *et al.* 2013), the degree of welding and flow thicknesses of the pre-basinal ignimbrites suggest that these rocks also possibly erupted from calderas within 50–100 km of the Cerocahui basin region that temporally overlap with the end of late Oligocene ignimbrite flare-up volcanism to the east, although more geochronologic data are needed to confirm this interpretation. There is no direct evidence of extensional deformation in the region of the Cerocahui basin during deposition of the silicic outflow ignimbrite sheets (Figure 11A), such as occurred during deposition of the upper (post-ca. 27.5 Ma) part of the ignimbrite section in the Guazapares Mining District region (Murray *et al.* 2013). However, given that the oldest age within the Cerocahui basin is from a thin non-welded ignimbrite interbedded with the Bahuichivo volcanics that overlie the Parajes formation near the Piedra Bola fault (28.1 ± 0.8 Ma), and this is the same age (within uncertainty) of the timing of the onset of extension to the west, extension in the Cerocahui basin region may have also begun during deposition of the youngest silicic outflow ignimbrites.

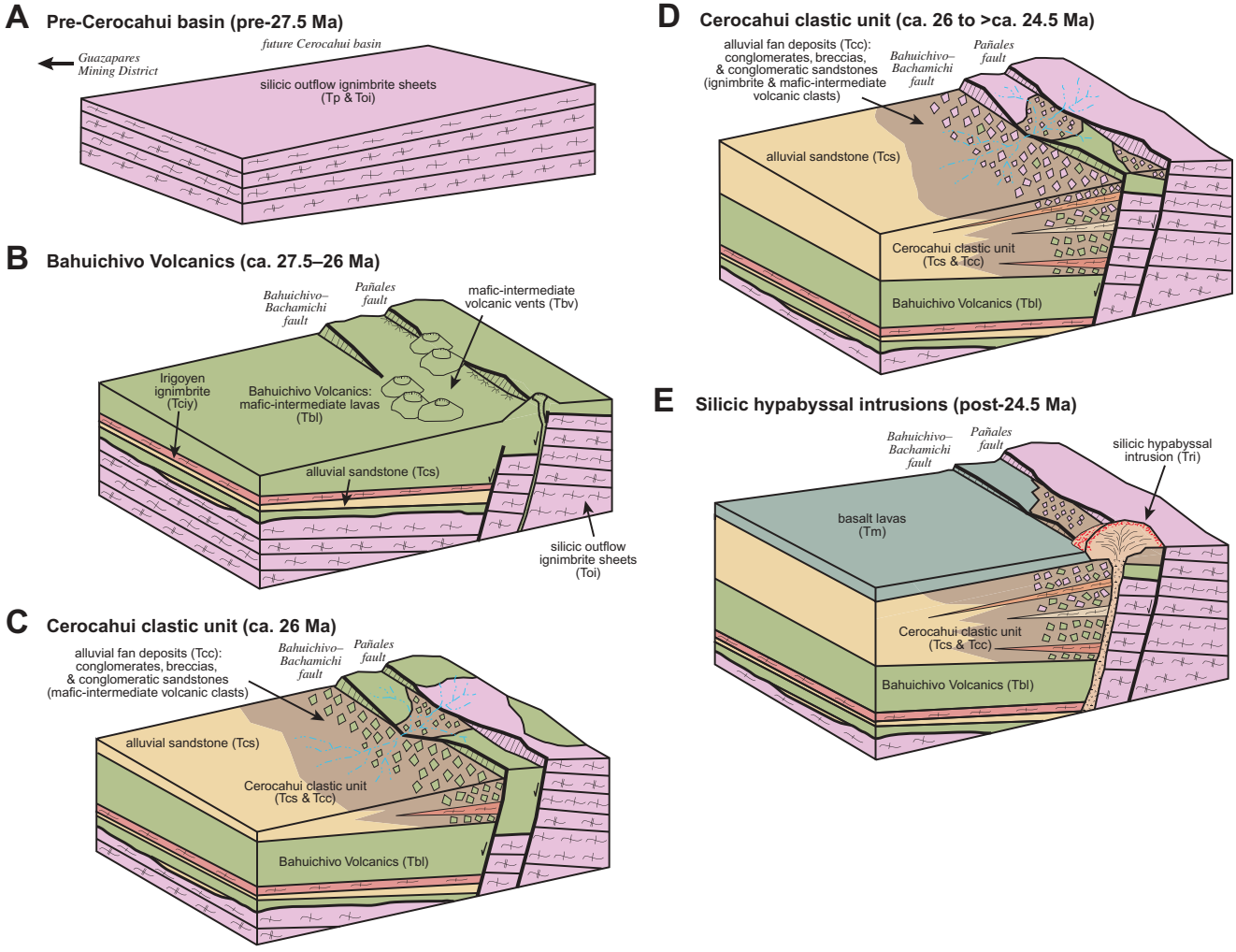

Figure 11. Schematic block diagrams illustrating the developmental history of the Cerocahui basin. The colours correspond to the map units in Figure 3. (A) Pre-basinal eruption of plateau-forming welded silicic outflow ignimbrites from distant (>50 km) sources, with sheets extending eastward from the Cerocahui basin and westward to the Guazapares Mining District region. (B) Initiation of crustal extension resulted in eruption of the Bahuichivo volcanics from fault-controlled vents, primarily along the eastern basin margin, into the Cerocahui basin and onto the basin-bounding footwall. The lavas of the Bahuichivo volcanics are interstratified with alluvial sandstone and the Irigoyen ignimbrite in the basin. (C) Extensional uplift related to continued motion of the basin-bounding normal faults triggers erosion of the Bahuichivo volcanics, with resulting mafic-intermediate volcanic-rich material (green clasts) deposited in the lower part of the Cerocahui clastic unit. (D) Further extensional deformation of the basin-bounding normal faults unroofs the older silicic outflow ignimbrites, resulting in mixed non-welded to welded silicic ignimbrite (pink clasts) and mafic-intermediate volcanic detritus (green clasts) deposited in the upper section of the Cerocahui clastic unit. (E) Eruption of the basalt lavas into the Cerocahui basin, followed by offset of the basalt lava unit across the Bahuichivo–Bachamichi fault. Silicic hypabyssal intrusions were emplaced along the basin-bounding Bahuichivo–Bachamichi fault and normal faults within the basin that offset older deposits.

Depositional relationships, growth strata, and subvolcanic intrusions that are likely fault-localized suggest that the Bahuichivo volcanics and Cerocahui clastic unit represent the synextensional growth of mafic-intermediate volcanic centres and volcaniclastic alluvial deposition in the Cerocahui basin during the late Oligocene (Figure 11B–11E). The alluvial fan deposits of the Cerocahui clastic unit likely formed a bajada along the eastern margin of the Cerocahui basin adjacent to the basin-bounding fault and prograded into the subsiding half-graben from the east and accumulated over the Bahuichivo volcanics (Figure 11C–11D).

The stratigraphic trend in conglomerate-breccia clast compositions in the Cerocahui clastic unit shows an upsection decrease in mafic-intermediate volcanic fragments and an upsection increase in welded and non-welded ignimbrite clasts, with fragments of silicic lava restricted to the lowest rocks of the section (Figure 7). The flow-banded silicic lava clasts suggest erosion of silicic volcanoes or plugs in the vicinity of the Cerocahui basin, as mafic-intermediate volcanic fragments are intermingled with the silicic lava clasts in the alluvial deposits; further study is needed to determine the source of these silicic lava clasts and its relative timing to the eruption of the Bahuichivo volcanics. The upsection trends in clast composition appear to record inverse stratigraphy related to unroofing of the active half-graben footwall block (Figures 7 and 11C–11D), with erosion of the Bahuichivo volcanics (Figure 11C) followed by erosion of the silicic outflow ignimbrite sheets (Figure 11D). The rocks on the footwall of the Bahuichivo–Bachamichi fault consist of silicic outflow ignimbrites, the Bahuichivo volcanics, and limited conglomerate and ignimbrite deposits of the Cerocahui clastic unit, whereas rocks on the footwall of the Pañales fault to the east are restricted to prebasinal silicic outflow ignimbrites; sedimentary and volcanic deposits related to the Cerocahui basin strata described above are not identified immediately east of this fault (Figure 3; Plate 1). This absence of Cerocahui basin fill supports the interpretation that extensional footwall uplift led to erosion of the Bahuichivo volcanics first, and then the underlying silicic outflow ignimbrites, with their erosional products deposited in the adjacent half-graben basin to the west (Figure 11C–11D).

Following deposition of the Cerocahui clastic unit, basalt lavas were erupted and ponded within the Cerocahui basin (Figure 11E). As noted above, these lavas are offset by the basin-bounding fault system, as well as by normal faults within the basin (Figures 3 and 4; Plate 1), suggesting synextensional volcanism. Younger silicic hypabyssal intrusions intruded along normal faults in the basin, suggesting that these pre-existing structures were utilized as pathways for magma accent and emplacement (Figure 11E).

Regional correlations

Based on similar lithology, timing of synextensional deposition, and proximity, the three stratigraphic subdivisions within the Cerocahui basin (Bahuichivo volcanics, Cerocahui clastic unit, and basalt lavas) are broadly correlative with the ca. 27–24.5 Ma Témoris formation in the Guazapares Mining District region (e.g. Murray *et al.* 2013) (Figure 12). Similar to the stratigraphy of the Cerocahui basin, the Témoris formation to the west is dominated by synextensional mafic-intermediate volcanic rocks and fault-localized intrusive equivalents, volcaniclastic alluvial fan deposits, and an upper section of interbedded alluvial deposits and distal silicic ignimbrites deposited above these mafic-intermediate lavas. However, there are much greater proportions of sandstones, conglomerates, and breccias in the Cerocahui basin than there are in the Témoris formation (Figure 12). In addition, the basalt lavas that cap the Cerocahui clastic unit are not present in the upper part of the Témoris formation to the west, although there basalt lavas are interbedded within the lower part of the formation (Murray *et al.* 2013) (Figure 12).

The sizes of half-graben basins in the Cerocahui and Guazapares Mining District regions also differ. Normal faults are more diffuse in the Guazapares Mining District region, with several closely spaced half-graben basins that are generally smaller (~1 to 4 km wide, 100 to >600 m deep) than the ~12 km-wide, >1200 m-deep Cerocahui basin (Figure 2). Perhaps this half-graben size difference is related to the geographic position of the Cerocahui basin immediately adjacent to the region defined as the unextended core of the Sierra Madre Occidental to the east, with the Cerocahui basin and Guazapares Mining District regions likely representing the eastern limit of the Gulf Extensional Province. The structures of the Cerocahui basin and the Guazapares Mining District region may represent the transition at the edge of the Gulf Extensional Province from the unextended core to the east, into the region of highly extended core-complexes to the west in Sonora.

The silicic hypabyssal intrusions in the Cerocahui basin are not dated directly, but they are tentatively correlated with the ca. 24.5–23 Ma Sierra Guazapares formation of the Guazapares Mining District region (e.g. Murray *et al.* 2013), which records the onset of local silicic flare-up-related magmatism ~20 km to the west during the onset of the early Miocene pulse of the ignimbrite flare-up. The Sierra Guazapares formation includes fault-localized fissure magmatism with silicic hypabyssal intrusions emplaced along pre-existing faults (Murray *et al.* 2013), similar to the fault-controlled silicic intrusions in the Cerocahui basin (Figure 11E). However, as noted above, in the Cerocahui basin, these intrusions do not pass upward into ignimbrites or lavas as they do in the Sierra

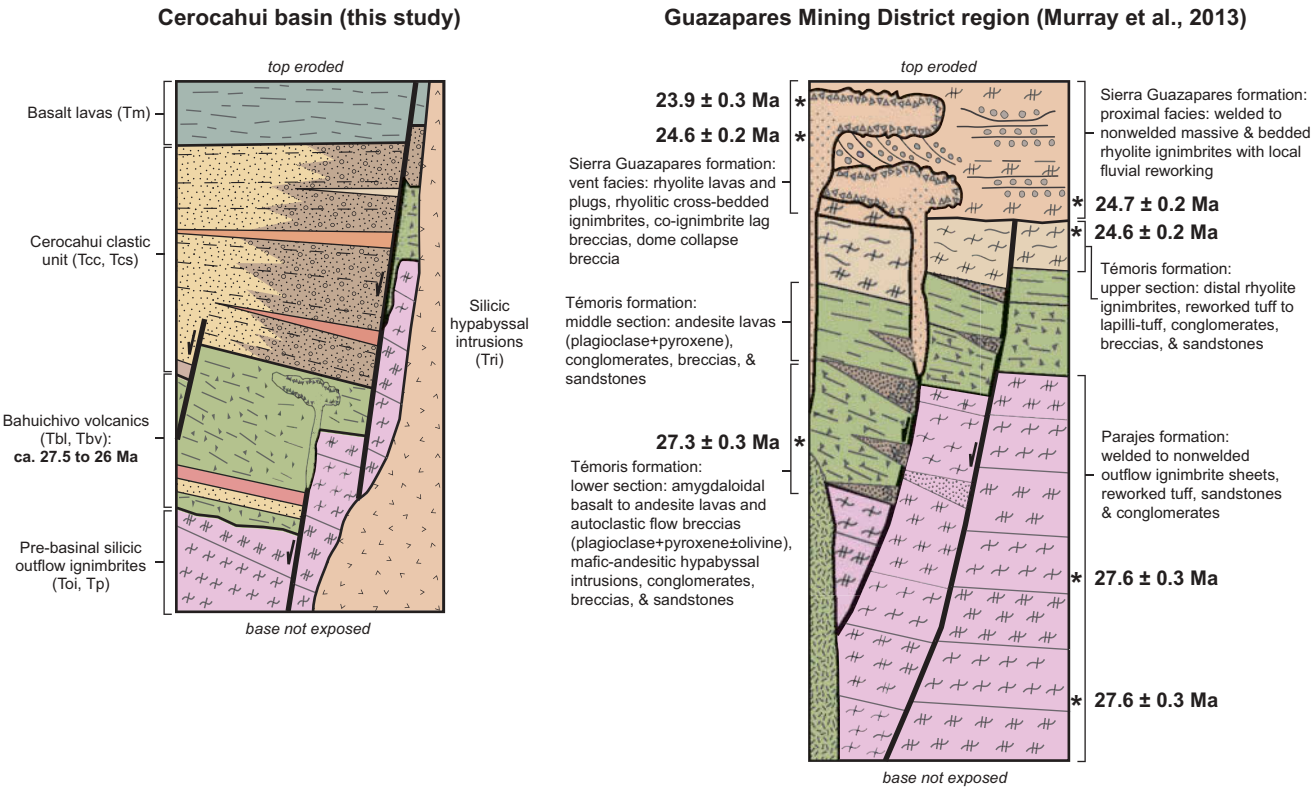

Figure 12. Generalized stratigraphic columns comparing the rocks of the Cerocahui basin (this study) to those of the Guazapares Mining District region, depicting the characteristics, depositional relationships, and ages of the Parajes formation, Témoris formation, and the Sierra Guazapares formation (after Murray *et al.* 2013).

Guazapares formation; it is not known whether this is an artefact of preservation (i.e. the top of the section is eroded), or whether silicic volcanism was minimal in the Cerocahui region.

The late Oligocene timing of volcanism and synextensional deposition in the Cerocahui basin is generally consistent with regional data patterns suggesting a post-ca. 40 Ma southwestward migration of arc-front magmatism across the Sierra Madre Occidental (e.g. Damon *et al.* 1981; Gans 1997; Gans *et al.* 2003; Ferrari et *al.* 2007; Henry *et al.* 2010). The ca. 27.5–26 Ma Bahuichivo volcanics post-date late Eocene to early Oligocene volcanism to the northeast of the study area, and are older than coeval with late Oligocene to early Miocene volcanism to the west in Sonora (Ferrari *et al.* 2007; Murray *et al.* 2013 and references therein). The late Oligocene age of extension of the Cerocahui basin and Guazapares Mining District region is roughly coeval with the onset of extension in the end Oligocene–early Miocene fault-bound grabens and core complexes located farther west in Sonora, although extension in this study area ended earlier than it did in the west (Gans 1997; McDowell *et al.* 1997; Wong *et al.* 2010; Murray *et al.* 2013 and references therein).

Conclusions

The rocks in the Cerocahui basin and adjacent Guazapares Mining District region record late Oligocene to early Miocene magmatism and synextensional deposition in the northern Sierra Madre Occidental. The oldest rocks in this region are silicic outflow ignimbrite sheets that erupted during the end of the early Oligocene pulse of the ignimbrite flare-up from sources likely to the east, representing medial outflow facies that were mostly deposited prior to development of the Cerocahui half-graben basin. These ignimbrites are likely correlative with the ca. 27.5 Ma Parajes formation immediately to the west in the Guazapares Mining District region, which suggests synextensional deposition of the youngest ignimbrites of the formation, and to ignimbrite sections described to the east by Swanson *et al.* (2006). The overlying synextensional deposits of the Cerocahui basin include: (1) the basal basin fill, consisting of the ca. 27.5–26 Ma Bahuichivo volcanics, mafic-intermediate lavas erupted from fault-localized synextensional volcanic centres primarily on the eastern half-graben margin; (2) the Cerocahui clastic unit, consisting largely of a bajada of alluvial fan-fluvial systems with minor interbedded distal

ignimbrites that prograded into the half-graben basin from the active eastern fault margin, and (3) a >300 m-thick section of basalt lavas ponded within, and restricted to, the Cerocahui basin. The mafic-intermediate volcanic and alluvial deposits of the Cerocahui basin are likely equivalent to the ca. 27–24.5 Ma Témoris formation in the Guazapares Mining District region and represent a period of the Southern Cordillera basaltic andesite (SCORBA) magmatism erupted after the early Oligocene ignimbrite pulse. Following deposition in the Cerocahui basin, silicic hypabyssal intrusions were emplaced along normal faults in the Cerocahui basin. These silicic intrusions are likely related to the ca. 24.5–23 Ma Sierra Guazapares formation in the Guazapares Mining District region, which were emplaced during the initiation of the early Miocene pulse of the ignimbrite flare-up. The late Oligocene to early Miocene timing of magmatism and synextensional deposition in the Cerocahui basin and Guazapares Mining District regions generally supports the regional interpretation that ignimbrite flare-up magmatism and crustal extension migrated southwestward with time.

Acknowledgements

Initial field studies of the Cerocahui basin (in 2005) were supported on Busby's personal funds in her 4WD vehicle, and were carried out with Profesora Elena Centeno-Garcia (Universidad Nacional Autónoma de México, UNAM), who had recognized this unusual red-bed succession on a previous trip in the Sierra Madre Occidental. Thanks are also due to Professor Terry Wright (CSU Sonoma, now deceased), who helped Busby and Centeno-Garcia with the initial fieldwork. Murray and Busby continued to study the basin with support from Paramount Gold & Silver Corp., arranged by Larry Segerstrom, Danny Sims, and Denis Norton, with assistance from Dana Durgin, Armando Valtierra, and Javier Martinez. Dana Roeber Murray and Jordan Lewis assisted in the field. Luigi Solari and Carlos Ortega-Obregón (Universidad Nacional Autónoma de México, UNAM) assisted with LA-ICP-MS analyses. Fieldwork by Murray and Verde Ramírez in 2010 was supported by a UC Mexus (University of California Institute for Mexico and the United States) grant to Busby and Centeno-García; Murray's geochronological work was also supported by that grant. National Science Foundation grant EAR-1019559 to Busby provided support to compile and write up the results. Additional financial support was provided by a Geological Society of America student research grant to Murray. Special thanks are due to Professor Emeritus Fred McDowell (University of Texas at Austin), for freely sharing his extensive knowledge of the Sierra Madre Occidental with Busby during her Visiting Professorship at UT Austin in 2010–2011. We thank Douglas Burbank, Phillip Gans, and John Cottle for a detailed informal review. Constructive formal reviews by Christopher Henry and Luca Ferrari and comments by John Wakabayashi and Robert J. Stern helped improve the manuscript.

Supplemental data

Supplemental data for this article can be accessed at http://dx.doi.org/10.1080/00206814.2014.941022.

References

Aguirre-Díaz, G.J., and Labarthe-Hernández, G., 2003, Fissure ignimbrites: Fissure-source origin for voluminous ignimbrites of the Sierra Madre Occidental and its relationship with Basin and Range faulting: Geology, v. 31, no. 9, p. 773–776. doi:10.1130/G19665.1

Aguirre-Díaz, G.J., and McDowell, F.W., 1991, The volcanic section at Nazas, Durango, Mexico, and the possibility of widespread Eocene volcanism within the Sierra Madre Occidental: Journal of Geophysical Research, v. 96, no. B8, p. 13373–13388. doi:10.1029/91JB00245

Aguirre-Díaz, G.J., and McDowell, F.W., 1993, Nature and timing of faulting and synextensional magmatism in the southern Basin and Range, central-eastern Durango, Mexico: Geological Society of America Bulletin, v. 105, p. 1435–1444. doi:10.1130/0016-7606(1993)105<1435:NATOFA>2.3.CO;2

Armstrong, R.L., and Ward, P.L., 1991, Evolving geographic patterns of Cenozoic magmatism in the North American Cordillera: The temporal and spatial association of magmatism and metamorphic core complexes: Journal of Geophysical Research, v. 96, no. B8, p. 13201–13224. doi:10.1029/91JB00412

Best, M.G., and Christiansen, E.H., 1991, Limited extension during peak Tertiary volcanism, Great Basin of Nevada and Utah: Journal of Geophysical Research, v. 96, p. 13509–13528. doi:10.1029/91JB00244

Best, M.G., Christiansen, E.H., and Gromme, S., 2013, Introduction: The 36-18 Ma southern Great Basin, USA, ignimbrite province and flareup: Swarms of subduction-related supervolcanoes: Geosphere, v. 9, p. 260–274. doi:10.1130/GES00870.1

Blair, T.C., and McPherson, J.G., 1994, Alluvial fans and their natural distinction from rivers based on morphology, hydraulic processes, sedimentary processes, and facies assemblages: Journal of Sedimentary Research, v. A64, no. 3, p. 450–489.

Bryan, S., 2007, Silicic large igneous provinces: Episodes, v. 30, no. 1, p. 1–12.

Bryan, S.E., and Ernst, R.E., 2008, Revised definition of Large Igneous Provinces (LIPs): Earth-Science Reviews, v. 86, p. 175–202. doi:10.1016/j.earscirev.2007.08.008

Bryan, S.E., and Ferrari, L., 2013, Large igneous provinces and silicic large igneous provinces: Progress in our understanding over the last 25 years: Geological Society of America Bulletin, v. 125, no. 7–8, p. 1053–1078. doi:10.1130/B30820.1

Bryan, S.E., Ferrari, L., Reiners, P.W., Allen, C.M., Petrone, C.M., Ramos-Rosique, A., and Campbell, I.H., 2008, New insights into crustal contributions to large-volume rhyolite generation in the mid-Tertiary Sierra Madre Occidental Province, Mexico, revealed by U-Pb geochronology: Journal of Petrology, v. 49, no. 1, p. 47–77. doi:10.1093/petrology/egm070

Bryan, S.E., Orozco-Esquivel, T., Ferrari, L., and López-Martínez, M., 2013, Pulling apart the mid to Late Cenozoic magmatic record of the Gulf of California: Is there a Comondú arc? *in* Gomez-Tuena, A., Straub, S.M., and Zellmer, G.F., eds., Orogenic andesites and crustal growth: Geological Society of London Special Publication, v. 385 doi:10.1144/SP385.8. http://sp.lyellcollection.org/content/early/2013/07/30/SP385.8.abstract

Bryan, S.E., Riley, T.R., Jerram, D.A., Leat, P.T., and Stephens, C.J., 2002, Silicic volcanism: An undervalued component of large igneous provinces and volcanic rifted margins, *in* Menzies, M.A., Klemperer, S.L., Ebinger, C.J., and Baker, J., eds., Volcanic rifted margins: Geological Society of America Special Paper, v. 362, p. 97–118.

Busby, C.J., 2013, Birth of a plate boundary at ca. 12 Ma in the Ancestral Cascades arc, Walker Lane belt of California and Nevada: Geosphere, v. 9, no. 5, p. 1147–1160. doi:10.1130/GES00928.1

Cameron, K.L., Nimz, G.J., Niemeyer, S., and Gunn, S., 1989, Southern Cordilleran basaltic andesite suite, southern Chihuahua, Mexico: A link between Tertiary continental arc and flood basalt magmatism in North America: Journal of Geophysical Research, v. 94, no. B6, p. 7817–7840. doi:10.1029/JB094iB06p07817

Cather, S.M., Dunbar, N.W., McDowell, F.W., McIntosh, W.C., and Scholle, P.A., 2009, Climate forcing by iron fertilization from repeated ignimbrite eruptions: The icehouse–silicic large igneous province (SLIP) hypothesis: Geosphere, v. 5, no. 3, p. 315–324. doi:10.1130/GES00188.1

Christiansen, R.L., and Yates, R.S., 1992, Post-Laramide geology of the western U.S. Cordillera, *in* Burchfiel, B.C., Lipman, P. W., and Zoback, M.L., eds., The Cordilleran Orogen: Conterminous U.S.: The Geology of North America, Decade of North American Geology, Volume G-3: Boulder, CO, Geological Society of America, p. 261–406.

Cochemé, J.J., and Demant, A., 1991, Geology of the Yécora area, northern Sierra Madre Occidental, Mexico, *in* Pérez-Segura, E., and Jacques-Ayala, C., eds., Studies in Sonoran geology: Geological Society of America Special Paper, v. 254, p. 81–94.

Collinson, J.D., 1996, Alluvial sediments, *in* Reading, H.G., ed., Sedimentary environments: Processes, facies and stratigraphy (third edition): Oxford, Blackwell Science, p. 37–82.

Coney, P.J., 1978, Mesozoic-Cenozoic Cordilleran plate tectonics, *in* Smith, R.B., and Eaton, G.P., eds., Cenozoic tectonics and regional geophysics of the Western Cordillera: Geological Society of America Memoir, Volume 152: Boulder, CO, Geological Society of America, p. 33–50.

Coney, P.J., and Reynolds, S.J., 1977, Cordilleran Benioff zones: Nature, v. 270, p. 403–406. doi:10.1038/270403a0

Costa, A., Gottsmann, J., Melnik, O., and Sparks, R.S.J., 2011, A stress-controlled mechanism for the intensity of very large magnitude explosive eruptions: Earth and Planetary Science Letters, v. 310, no. 1–2, p. 161–166. doi:10.1016/j.epsl.2011.07.024

Damon, P.E., Shafiqullah, M., and Clark, K.F., 1981, Age trends of igneous activity in relation to metallogenesis in the southern Cordillera: Arizona Geological Society Digest, v. 14, p. 137–154.

DeCelles, P.G., Langford, R.P., and Schwartz, R.K., 1983, Two new methods of paleocurrent determination from trough cross-stratification: Journal of Sedimentary Petrology, v. 53, p. 629–642.

Dickinson, W.R., 2002, The Basin and Range Province as a composite extensional domain: International Geology Review, v. 44, p. 1–38. doi:10.2747/0020-6814.44.1.1

Dickinson, W.R., 2006, Geotectonic evolution of the Great Basin: Geosphere, v. 2, no. 7, p. 353–368. doi:10.1130/GES00054.1

Dickinson, W.R., 2013, Phanerozoic palinspastic reconstructions of Great Basin geotectonics (Nevada-Utah, USA): Geosphere, v. 9, no. 5, p. 1384–1396. doi:10.1130/GES00888.1

Dickinson, W.R., and Snyder, W.S., 1978, Plate tectonics of the Laramide orogeny, *in* Matthews, V., ed., Laramide folding associated with basement block faulting in the Western United States: Geological Society of America Memoir 151, p. 355–366.

Dreier, J., 1984, Regional tectonic control of epithermal veins in the Western United States and Mexico, *in* Wilkins, J., ed., Gold and silver deposits of the Basin and Range Province, Western U.S. A.: Arizona Geological Society Digest 15, p. 28–50.

Ferrari, L., López-Martínez, M., Orozco-Esquivel, T., Bryan, S. E., Duque-Trujillo, J., Lonsdale, P., and Solari, L., 2013, Late Oligocene to Middle Miocene rifting and synextensional magmatism in the southwestern Sierra Madre Occidental, Mexico: The beginning of the Gulf of California rift: Geosphere, v. 9, no. 5, p. 1161–1200. doi:10.1130/GES00925.1

Ferrari, L., López-Martínez, M., and Rosas-Elguera, J., 2002, Ignimbrite flare-up and deformation in the southern Sierra Madre Occidental, western Mexico: Implications for the late subduction history of the Farallon plate: Tectonics, v. 21, no. 4, p. 17-1–17-24. doi:10.1029/2001TC001302

Ferrari, L., Valencia-Moreno, M., and Bryan, S., 2007, Magmatism and tectonics of the Sierra Madre Occidental and its relation with the evolution of the western margin of North America, *in* Alaniz-Álvarez, S.A., and Nieto-Samaniego, Á.F., eds., Geology of México: Celebrating the centenary of the Geological Society of México: Geological Society of America Special Paper, v. 422, p. 1–39.

Gans, P.B., 1997, Large-magnitude Oligo-Miocene extension in southern Sonora: Implications for the tectonic evolution of northwest Mexico: Tectonics, v. 16, p. 388–408. doi:10.1029/97TC00496

Gans, P.B., Blair, K.D., MacMillan, I., Wong, M.S., and Roldán-Quintana, J., 2003, Structural and magmatic evolution of the Sonoran rifted margin: A preliminary report: Geological Society of America Abstracts with Programs, v. 35, no. 4, p. 21.

González León, C.M., McIntosh, W.C., Lozano-Santacruz, R., Valencia-Moreno, M., Amaya-Martínez, R., and Rodríguez-Castañeda, J.L., 2000, Cretaceous and Tertiary sedimentary, magmatic, and tectonic evolution of north-central Sonora (Arizpe and Bacanuchi Quadrangles), northwest Mexico: Geological Society of America Bulletin, v. 112, no. 4, p. 600–610. doi:10.1130/0016-7606(2000)112<600:CATSMA>2.0.CO;2

Grijalva-Noriega, F.J., and Roldán-Quintana, J., 1998, An overview of the Cenozoic tectonic and magmatic evolution of Sonora, northwestern Mexico: Revista Mexicana De Ciencias, v. 15, no. 2, p. 145–156.

Henry, C.D., and Aranda-Gomez, J.J., 2000, Plate interactions control middle-late Miocene, proto-Gulf and Basin and Range extension in the southern Basin and Range: Tectonophysics, v. 318, p. 1–26. doi:10.1016/S0040-1951(99)00304-2

Henry, C.D., McIntosh, W., McDowell, F.W., Lipman, P.W., Chapin, C.E., and Richardson, M.T., 2010, Distribution, timing, and controls of the mid-Cenozoic ignimbrite flareup in western North America: Geological Society of America Abstracts with Programs, v. 42, no. 5, p. 144.

Henry, C.D., McIntosh, W.C., McDowell, F.W., Lipman, P.W., and Chapin, C.E., 2012, The Cenozoic ignimbrite flareup in western North America: Distribution, timing, volume, and tectonic relations: Geological Society of America Abstracts with Programs, v. 44, no. 3, p. 21.

Hildreth, W., 1981, Gradients in silicic magma chambers: Implications for lithospheric magmatism: Journal of Geophysical Research, v. 86, no. B11, p. 10153–10192. doi:10.1029/JB086iB11p10153

Kelly, S.B., and Olsen, H., 1993, Terminal fans – A review with reference to Devonian examples: Sedimentary Geology, v. 85, p. 339–374. doi:10.1016/0037-0738(93)90092-J

Lipman, P.W., 2007, Incremental assembly and prolonged consolidation of Cordilleran magma chambers: Evidence from

the Southern Rocky Mountain volcanic field: Geosphere, v. 3, no. 1, p. 42–70. doi:10.1130/GES00061.1

Ludwig, K.L., 2008, Isoplot 3.70. A geochronological toolkit for Microsoft Excel: Berkeley Geochronology Center Special Publication No. 4, p. 1–77.

Luhr, J.F., Henry, C.D., Housh, T.B., Aranda-Gómez, J.J., and McIntosh, W.C., 2001, Early extension and associated mafic alkalic volcanism from the southern Basin and Range Province: Geology and petrology of the Rodeo and Nazas volcanic fields, Durango, México: Geological Society of America Bulletin, v. 113, p. 760–773. doi:10.1130/0016-7606(2001)113<0760:EEAAMA>2.0.CO;2

McDowell, F.W., 2007, Geologic transect across the northern Sierra Madre Occidental volcanic field, Chihuahua and Sonora, Mexico: Geological Society of America Digital Map and Chart Series, v. 6, p. 70.

McDowell, F.W., 2012, Timing of intense magmatic episodes in the northern and central Sierra Madre Occidental, western Mexico: Geological Society of America Abstracts with Programs, v. 44, no. 3, p. 21.

McDowell, F.W., and Clabaugh, S.E., 1979, Ignimbrites of the Sierra Madre Occidental and their relation to the tectonic history of western Mexico, *in* Chapin, C.E., and Elston, W. E., eds., Ash-Flow Tuffs: Geological Society of America Special Paper, v. 180, p. 113–124.

McDowell, F.W., and Keizer, R.P., 1977, Timing of mid-Tertiary volcanism in the Sierra Madre Occidental between Durango City and Mazatlan, Mexico: Geological Society of America Bulletin, v. 88, p. 1479–1487. doi:10.1130/0016-7606(1977)88<1479:TOMVIT>2.0.CO;2

McDowell, F.W., and Mauger, R.L., 1994, K-Ar and U-Pb zircon chronology of Late Cretaceous and Tertiary magmatism in central Chihuahua State, Mexico: Geological Society of America Bulletin, v. 106, p. 118–132. doi:10.1130/0016-7606(1994)106<0118:KAAUPZ>2.3.CO;2

McDowell, F.W., and McIntosh, W.C., 2012, Timing of intense magmatic episodes in the northern and central Sierra Madre Occidental: Western Mexico: Geosphere, v. 8, no. 6, p. 1502–1526.

McDowell, F.W., Roldán-Quintana, J., and Amaya-Martínez, R., 1997, Interrelationship of sedimentary and volcanic deposits associated with Tertiary extension in Sonora, Mexico: Geological Society of America Bulletin, v. 109, no. 10, p. 1349–1360. doi:10.1130/0016-7606(1997)109<1349:IOSAVD>2.3.CO;2

McQuarrie, N., and Oskin, M., 2010, Palinspastic restoration of NAVDat and implications for the origin of magmatism in southwestern North America: Journal of Geophysical Research, v. 115, no. B10401, doi:10.1029/2009JB006435

Miall, A.D., 1985, Architectural-element analysis: A new method of facies analysis applied to fluvial deposits: Earth-Science Reviews, v. 22, p. 261–308. doi:10.1016/0012-8252(85)90001-7

Minjárez Sosa, I., Montaño Jiménez, T.R., Ochoa Granillo, J.A., Grijalva Noriega, F.J., Ochoa Landín, L.H., Herrera Urbina, S., Guzmán Espinosa, J.B., and Mancilla Gutiérrez, A.A., 2002, Carta Geológico-Minera Ciudad Obregón G12-3 Sonora, Chihuahua y Sinaloa: Servicio Geológico Mexicano, scale 1:250,000.

Murray, B.P., Busby, C.J., Ferrari, L., and Solari, L.A., 2013, Synvolcanic crustal extension during the mid-Cenozoic ignimbrite flare-up in the northern Sierra Madre Occidental, Mexico: Evidence from the Guazapares Mining District region, western Chihuahua: Geosphere, v. 9, no. 5, p. 1201–1235. doi:10.1130/GES00862.1

Murray, B.P., Horton, B.K., Matos, R., and Heizler, M.T., 2010, Oligocene–Miocene basin evolution in the northern Altiplano, Bolivia: Implications for evolution of the central Andean backthrust belt and high plateau: Geological Society of America Bulletin, v. 122, no. 9–10, p. 1443–1462. doi:10.1130/B30129.1

Nieto-Samaniego, Á.F., Ferrari, L., Alaniz-Alvarez, S.A., Labarthe-Hernández, G., and Rosas-Elguera, J., 1999, Variation of Cenozoic extension and volcanism across the southern Sierra Madre Occidental volcanic province, Mexico: Geological Society of America Bulletin, v. 111, no. 3, p. 347–363. doi:10.1130/0016-7606(1999)111<0347:VOCEAV>2.3.CO;2

Ramírez Tello, E., and Garcia Peralta, Á.A., 2004, Carta Geológico-Minera Témoris G12-B39 Chihuahua: Servicio Geológico Mexicano, scale 1:50,000.

Sambridge, M.S., and Compston, W., 1994, Mixture modeling of multi-component data sets with application to ion-probe zircon ages: Earth and Planetary Science Letters, v. 128, p. 373–390. doi:10.1016/0012-821X(94)90157-0

Swanson, E.R., Kempter, K.A., McDowell, F.W., and McIntosh, W.C., 2006, Major ignimbrites and volcanic centers of the Copper Canyon area: A view into the core of Mexico's Sierra Madre Occidental: Geosphere, v. 2, no. 3, p. 125–141. doi:10.1130/GES00042.1

Swanson, E.R., and McDowell, F.W., 1984, Calderas of the Sierra Madre Occidental volcanic field, western Mexico: Journal of Geophysical Research, v. 89, p. 8787–8799. doi:10.1029/JB089iB10p08787

Swanson, E.R., and McDowell, F.W., 1985, Geology and geochronology of the Tomochic caldera, Chihuahua, Mexico: Geological Society of America Bulletin, v. 96, p. 1477–1482. doi:10.1130/0016-7606(1985)96<1477:GAGOTT>2.0.CO;2

Uba, C.E., Heubeck, C., and Hulka, C., 2005, Facies analysis and basin architecture of the Neogene Subandean synorogenic wedge, southern Bolivia: Sedimentary Geology, v. 180, p. 91–123. doi:10.1016/j.sedgeo.2005.06.013

Ward, P.L., 1991, On plate tectonics and the geologic evolution of southwestern North America: Journal of Geophysical Research, v. 96, no. B7, p. 12479–12496. doi:10.1029/91JB00606

Wark, D.A., Kempter, K.A., and McDowell, F.W., 1990, Evolution of waning subduction-related magmatism, northern Sierra Madre Occidental, Mexico: Geological Society of America Bulletin, v. 102, p. 1555–1564. doi:10.1130/0016-7606(1990)102<1555:EOWSRM>2.3.CO;2

Wong, M.S., Gans, P.B., and Scheier, J., 2010, The $^{40}Ar/^{39}Ar$ thermochronology of core complexes and other basement rocks in Sonora, Mexico: Implications for Cenozoic tectonic evolution of northwestern Mexico: Journal of Geophysical Research, v. 115, no. B07414. doi:10.1029/2009JB007032